Summary of part IV

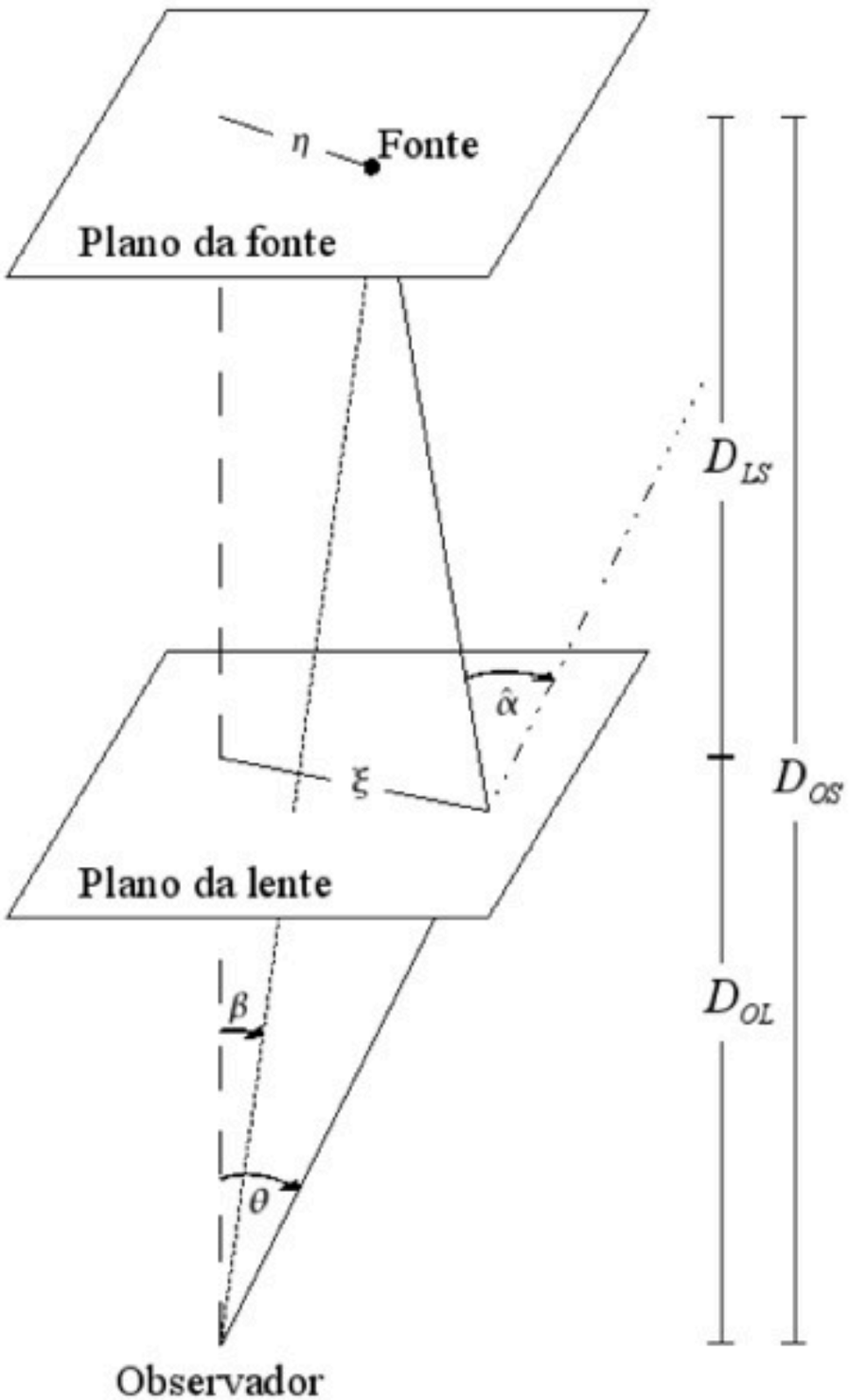

Lens equation $\vec{\beta} = \vec{\theta} - \vec{\alpha}\left(\vec{\theta}\right)$

$= \vec{\theta} - \vec{\nabla}_\theta \Psi\left(\vec{\theta}\right)$

Lens potential $\Psi(\vec{x}) \equiv \frac{2}{c^2}\frac{D_{LS}}{D_{OS}D_{OL}}\psi$

Deflection angle

$$\hat{\vec{\alpha}} = \frac{4G}{c^2}\int d^2\xi' \Sigma\left(\vec{\xi}'\right)\frac{\vec{\xi} - \vec{\xi}'}{|\vec{\xi} - \vec{\xi}'|^2}$$

Multiple images, magnification,
Einstein rings, arcs
Examples: point mass, SIS

Singular Isothermal Sphere

Deflection angle

$$\hat{\vec{\alpha}} = 4\pi \left(\frac{\sigma_v}{c}\right)^2 \hat{\xi}$$

$$\Rightarrow \boxed{\theta = \theta_E - \beta}$$

$$\Rightarrow \boxed{\theta = \beta + \theta_E}$$

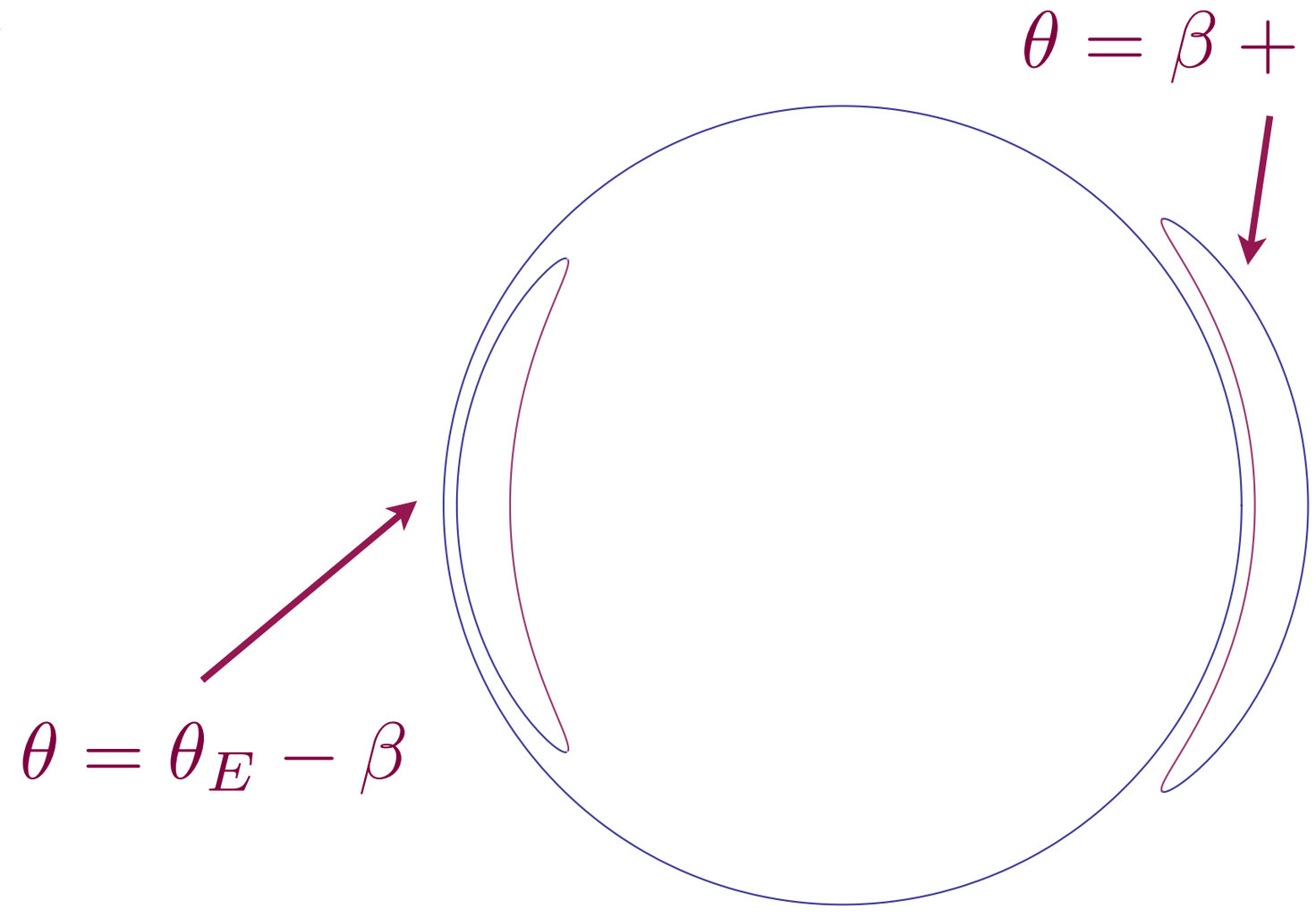

© Copyleft Martín Makler

Lensing Mapping

- image → source mapping:

$$\frac{\partial \beta_i}{\partial \theta_j} = \delta_{ij} - \frac{\partial^2 \Psi\left(\vec{\theta}\right)}{\partial \theta_i \partial \theta_j}$$

- single plane lensing

$$\Psi = \frac{2}{c^2} \frac{D_{LS}}{D_{OS} D_{OL}} \int \phi\left(\xi, z\right) dz$$

gravitational potential (astrophysics)

cosmological distances (cosmology)

$$D_{LS} = D_A\left(z_L, z_S\right)...$$

- eigenvalues:

$$\mu_1 = \frac{1}{1 - \kappa + \gamma}, \mu_2 = \frac{1}{1 - \kappa - \gamma}$$

- local magnification and axial ratio:

$$\mu = \mu_1 \, \mu_2$$

$$r = \left| \frac{\mu_1}{\mu_2} \right|$$

Lensing Mapping

- image → source mapping:

$$\frac{\partial \beta_i}{\partial \theta_j} = \delta_{ij} - \frac{\partial^2 \Psi\left(\vec{\theta}\right)}{\partial \theta_i \partial \theta_j}$$

- eigenvalues:

$$\mu_1 = \frac{1}{1-\kappa+\gamma}, \mu_2 = \frac{1}{1-\kappa-\gamma}$$

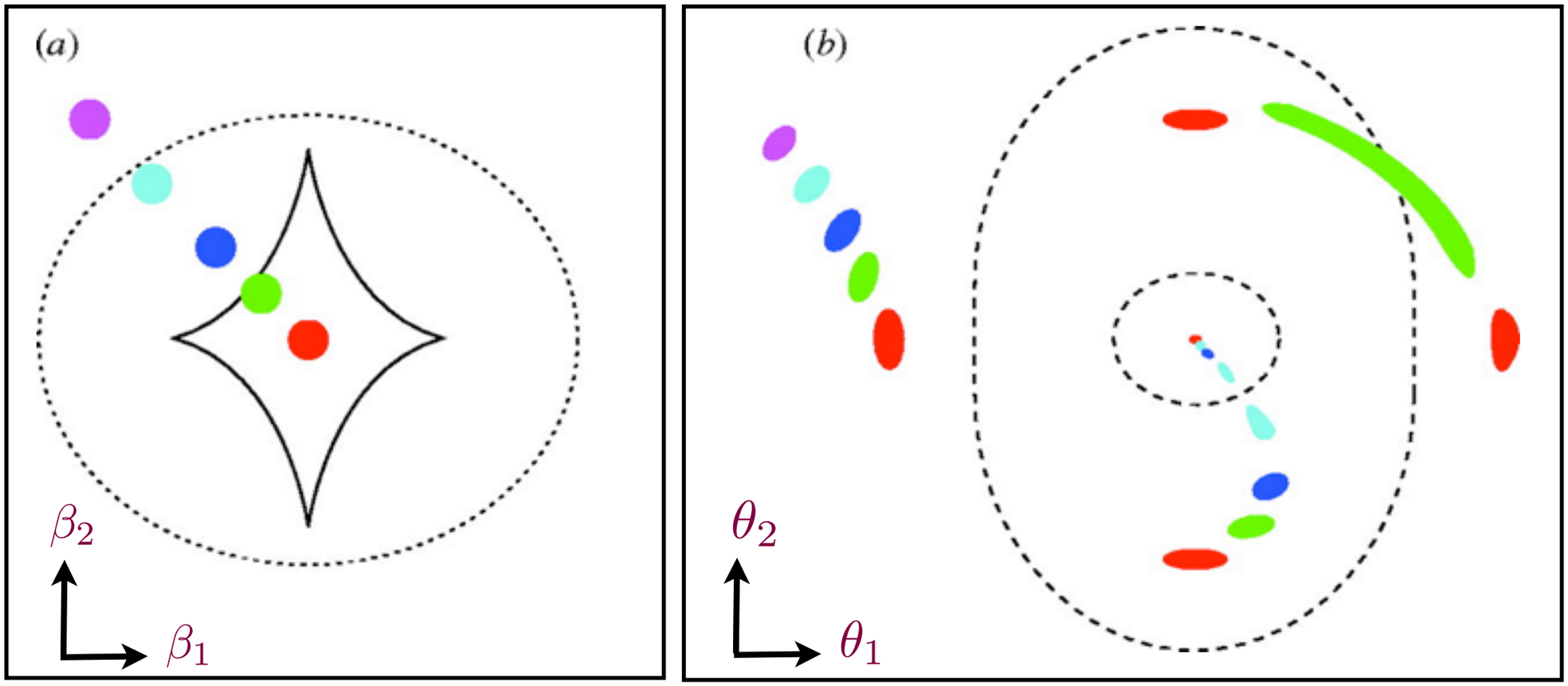

Source plane

Lens/image

Comportamento geral

Cáusticas:

- tangencial: astróides com cúspides
- radial: "oval"

Curvas críticas:

- tangencial: "oval"
- radial: "circular"

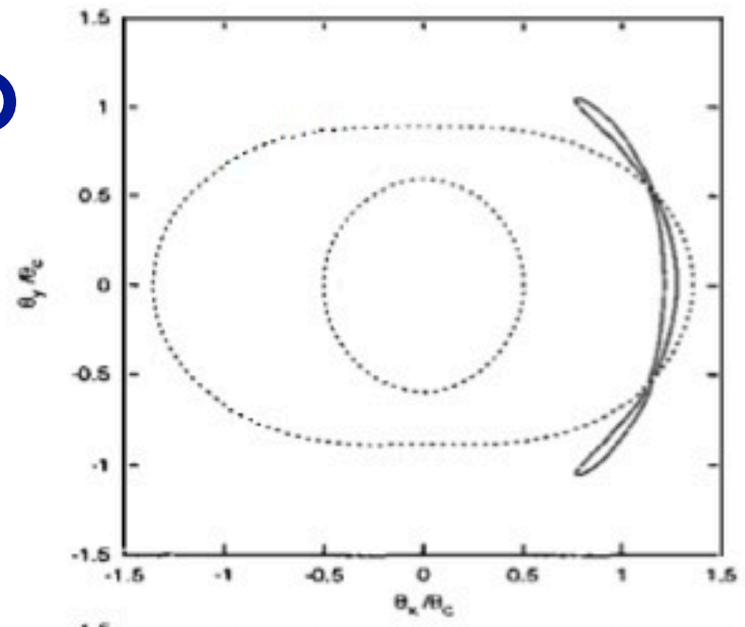

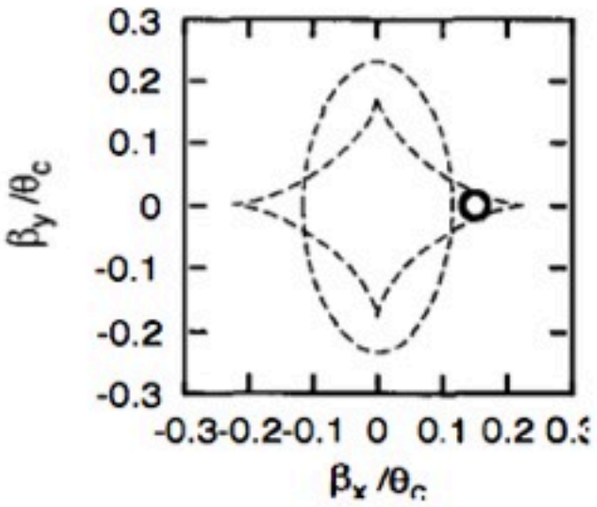

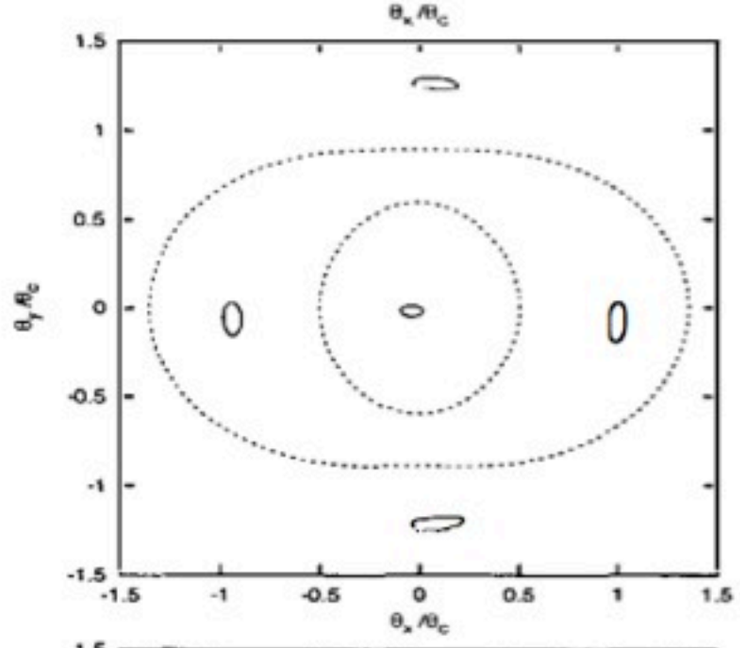

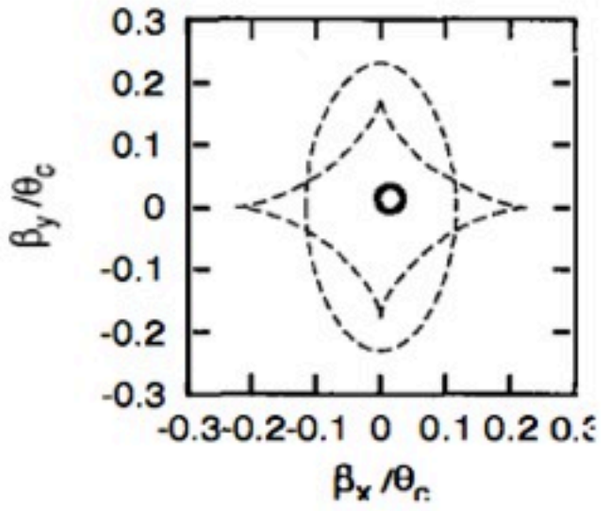

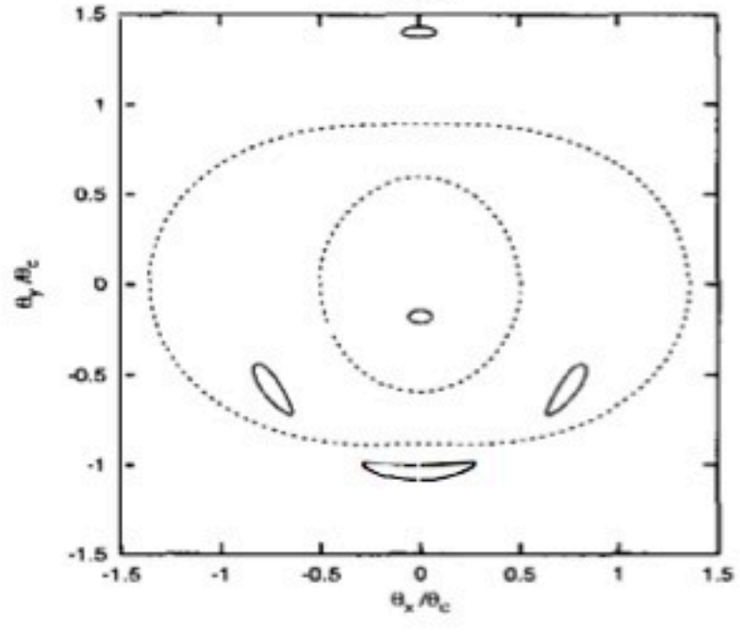

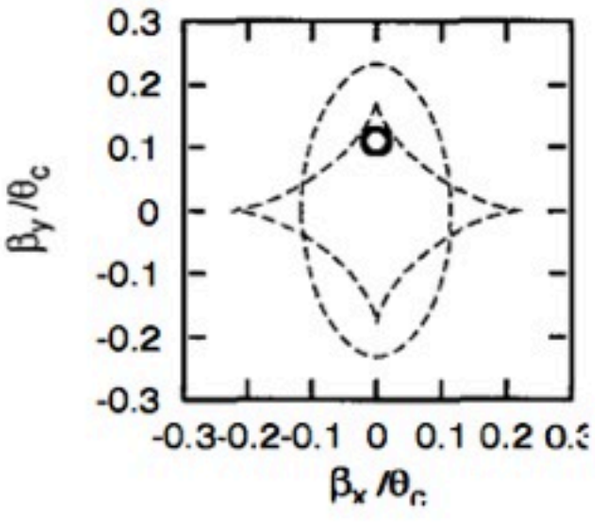

Arcos em modelos elípticos

Soluções analíticas para esfera isotérmica elíptica e pseudo-elíptica com campos externos e fontes elípticas

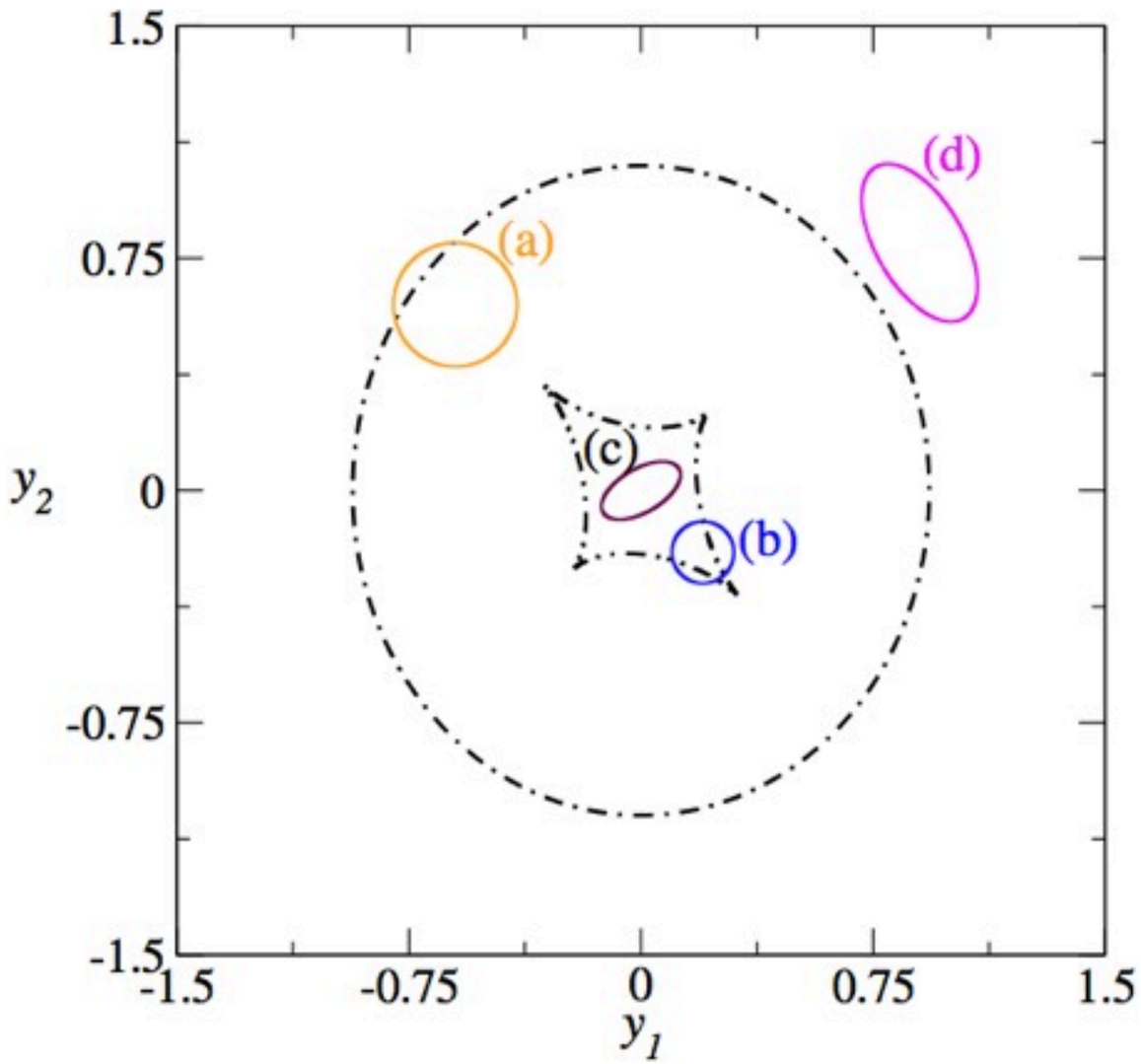

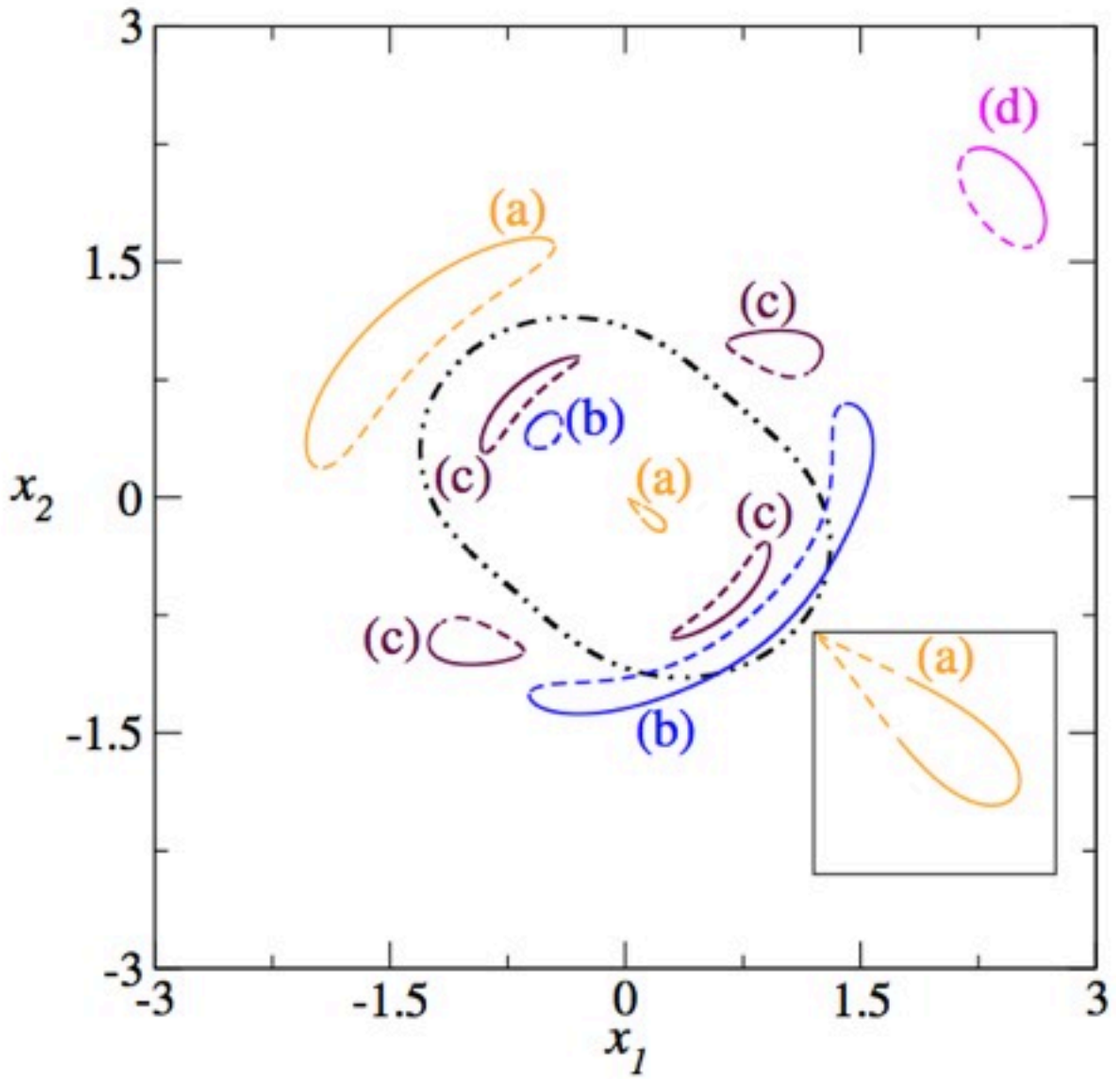

Dúmet-Montoya & Makler in prep.

Inverse Modeling: Mapping the Mass

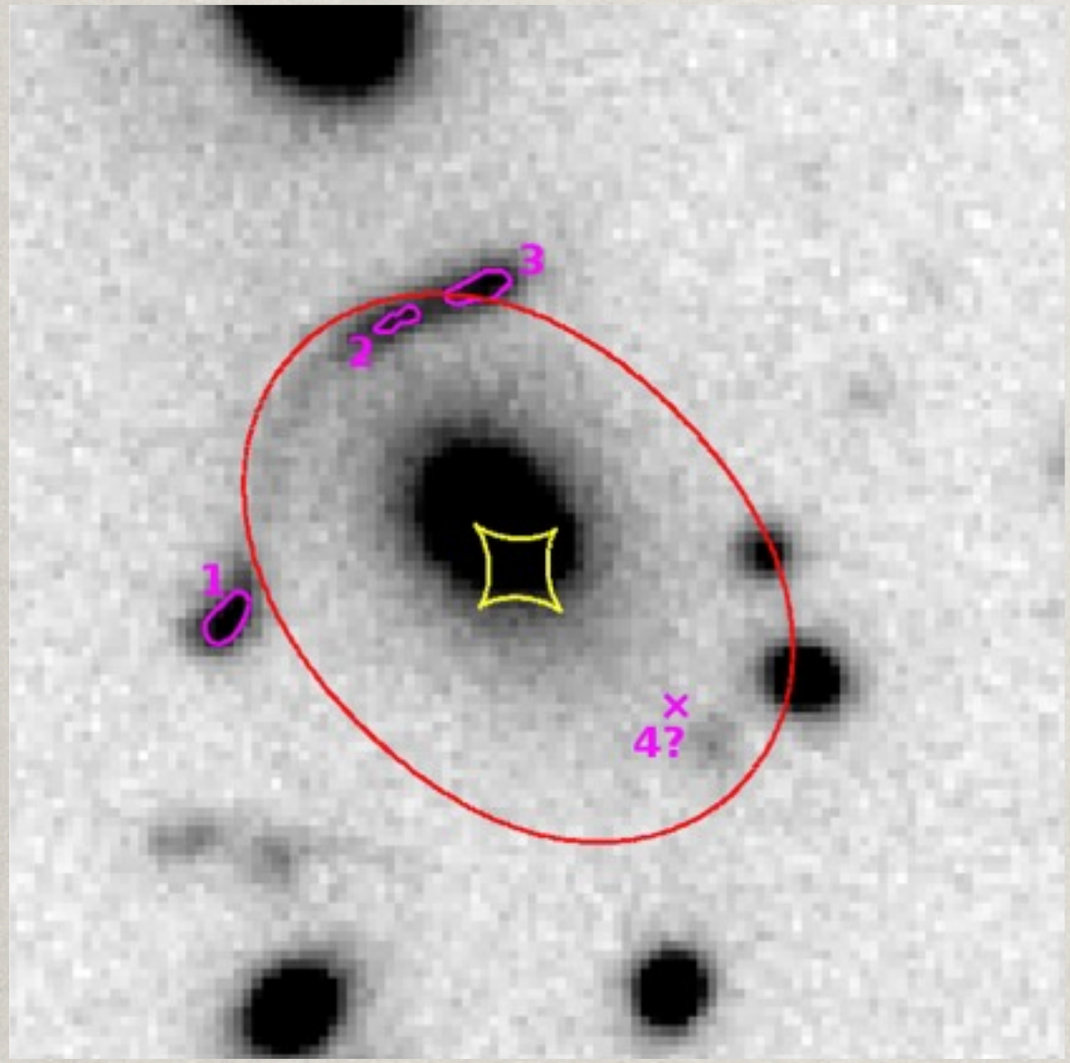

Use systems of multiple images to determine the lensing potential

$$\chi^2_{\rm lente} := \sum_i \left(\frac{\vec{\theta}_i^{\rm obs} - \vec{\theta}^{\rm mod}\left(\vec{\beta}, \vec{\Pi}\right)}{\sigma_i^{\rm obs}} \right)^2$$

Multiple image positions

Error on image positions

Methods: parametric (often "mass traces light"), free form

The more multiple images, the more constrains

Cluster x Galaxy scales

- Combination with independent mass constraints (e.g., x-ray, Sunyaev Zel'dovich, velocity dispersions) yields limits on cosmology or gravity

Regimes and Challenges

- Galaxy cluster scale
  - Complex mass models, but many families of multiple images
  - HST Data: Frontier Fields, CLASH, RELICS, etc.
  - + Massive spectroscopic follow-up (IFU/MUSE)
  - Cosmology from single systems + high-z sources
  - Limited to very massive lenses and few systems
  - Promising for particle DM properties!
- Galaxy scale systems
  - Simple mass modes, but few constraints
  - Also HST imaging, but few IFU data (e.g. Gemini/NIFS)
  - Promising for Modified Gravity!
- Statistics
  - Spin-off from cosmological surveys:

    $\mathcal{O}(10^{1\text{-}2}) \rightarrow \mathcal{O}(10^{3\text{-}5})$
  - Need to find these systems!
    - Automated arc finders
  - Understand selection function.
    - Use simulations
  - Need to automate analyses!
- Challenge: Systematics
  - Use simulations → end-to-end approach
  - Test modeling at the data level. Independent tests: predictions x SN!
  - Improve models from data: LSS/los, IFU, etc.

THE *HST* FRONTIER FIELDS

THE DEEPEST DATA EVER OBTAINED FOR LENSING GALAXY CLUSTERS !!!

Abell 2744 - z = 0.308
Fully observed

Atek et al. 2014a, ApJ, 786, 60 ; Laporte et al. 2014, A&A, 562, 8; Zitrin et al. 2014, ApJ, 793, 12; Ishigaki et al. 2015, ApJ, 799, 12; Atek et al. 2015, ApJ, 800, 18; Jauzac et al. 2015, MNRAS, 452, 437 ; Wang et al., ApJ, 811, 29

MACS J0416 - z = 0.396
Fully observed

Jauzac et al. 2014, MNRAS, 443, 1549; Lam et al. 2014, ApJ, 797, 98; Jauzac et al. 2015, MNRAS, 446 4132; Grillo et al. 2015, ApJ, 800, 38 ; Harvey et al. 2016, MNRAS, 458, 660 ; Caminha et al., 2016, arXiv1607.0346

MACS J1149 - z = 0.543
Fully observed
Kelly et al. 2015, *Science, 347, 1123 ;* Sharon & Johnson 2015, *ApJ, 800, 26 ;* Oguri 2015, *MNRAS, 449, 86 ;* Diego et al. 2016, MNRAS, 459, 344 ; Jauzac et al. 2016, MNRAS, 457, 2029 ; Treu et al. 2016, ApJ, 817, 60 ; Grillo et al. 2016, ApJ, 822, 78

MACS J0717 - z = 0.545
Fully observed
Diego et al. 2015, MNRAS, 451, 3920 ; Limousin et al. 2016, A&A, 588, 99; Kawamata et al. 2016, ApJ, 819, 14

Abell 370 - z = 0.375
ACS to go

Abell S1063 - z = 0.348
Fully observed
Diego et al. 2016, MNRAS 459, 3447



Testing for Systematics
Supernovae in MACS J1149.6+2223



Use prediction for the appearance of multiple images of the SN to test the models

When Refsdal meets Popper!

Draft version March 7, 2016
Preprint typeset using LaTeX style emulateapj v. 5/2/11

THE STORY OF SUPERNOVA 'REFSDAL' TOLD BY MUSE*

C. Grillo[1], W. Karman[2], S. H. Suyu[3], P. Rosati[4], I. Balestra[5], A. Mercurio[6], M. Lombardi[7], T. Treu[8], G. B. Caminha[4], A. Halkola, S. A. Rodney[9,10,11], R. Gavazzi[12], K. I. Caputi[2]

Draft version March 7, 2016

ABSTRACT

We present Multi Unit Spectroscopic Explorer (MUSE) observations in the core of the Hubble Frontier Fields (HFF) galaxy cluster MACS J1149.5+2223, where the first magnified and spatially-resolved multiple images of supernova (SN) 'Refsdal' at redshift 1.489 were detected. Thanks to a Director's Discretionary Time program with the Very Large Telescope and the extraordinary efficiency of MUSE, we measure 117 secure redshifts with just 4.8 hours of total integration time on a single 1 arcmin^2 target pointing. We spectroscopically confirm 68 galaxy cluster members, with redshift values ranging from 0.5272 to 0.5660, and 18 multiple images belonging to 7 background, lensed sources distributed in redshifts between 1.240 and 3.703. Starting from the combination of our catalog with those obtained from extensive spectroscopic and photometric campaigns using the *Hubble Space Telescope*, we select a sample of 300 (164 spectroscopic and 136 photometric) cluster members, within approximately 500 kpc from the brightest cluster galaxy, and a set of 88 reliable multiple images associated to 10 different background source galaxies and 18 distinct knots in the spiral galaxy hosting SN 'Refsdal'. We exploit this valuable information to build 6 detailed strong lensing models, the best of which reproduces the observed positions of the multiple images with a root-mean-square offset of only 0.26″. We use these models to quantify the statistical and systematic errors on the predicted values of magnification and time delay of the next emerging image of SN 'Refsdal'. We find that its peak luminosity should occur between March and June 2016, and should be approximately 20% fainter than the dimmest (S4) of the previously detected images but above the detection limit of the planned *HST*/WFC3 follow-up. We present our two-dimensional reconstruction of the cluster mass density distribution and of the SN 'Refsdal' host galaxy surface brightness distribution. We outline the roadmap towards even better strong lensing models with a synergetic MUSE and *HST* effort.

Subject headings: gravitational lensing – galaxies: clusters: general – galaxies: clusters: individuals: MACS J1149.5+2223 – Dark matter

"REFSDAL" MEETS POPPER: COMPARING PREDICTIONS OF THE RE-APPEARANCE OF THE MULTIPLY IMAGED SUPERNOVA BEHIND MACSJ1149.5+2223

T. Treu[1,28], G. Brammer[2], J. M. Diego[3], C. Grillo[4], P. L. Kelly[5], M. Oguri[6,7,8]
K. Sharon[12], A. Zitrin[13,29] Show full author list

Published 2016 January 20 • © 2016. The American Astronomical Society. All right
The Astrophysical Journal, Volume 817, Number 1

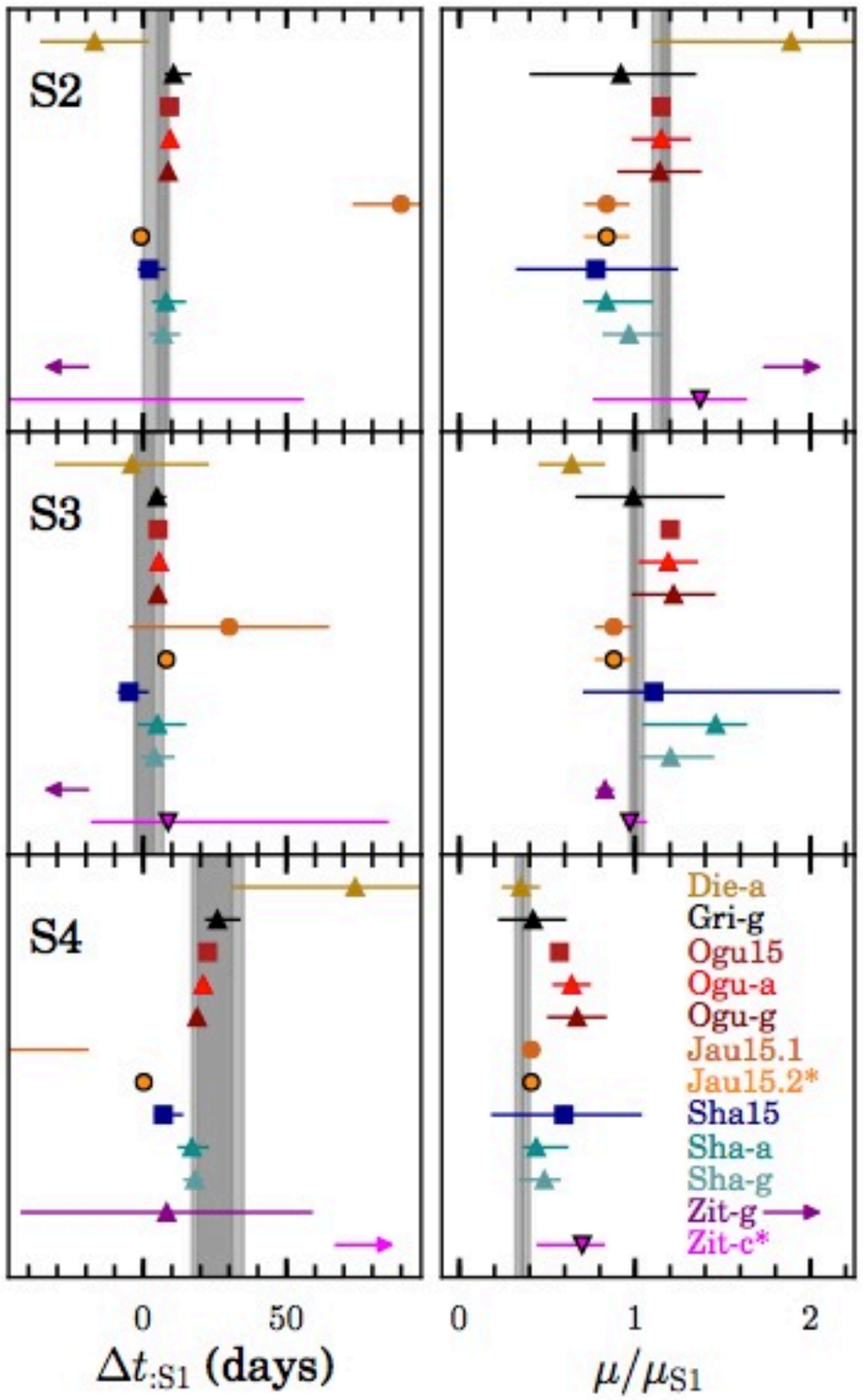

A free-form prediction for the reappearance of supernova Refsdal in the Hubble Frontier Fields cluster MACSJ1149.5+2223

Jose M. Diego,[1]★ Tom Broadhurst,[2,3] Cuncheng Chen,[4] Jeremy Lim,[4] Adi Zitrin,[5]†
Brian Chan,[4] Dan Coe,[6] Holland C. Ford,[6] Daniel Lam[4] and Wei Zheng[6]

[1]*IFCA, Instituto de Física de Cantabria (UC-CSIC), Av. de Los Castros s/n, E-39005 Santander, Spain*
[2]*Fisika Teorikoa, Zientzia eta Teknologia Fakultatea, Euskal Herriko Unibertsitatea UPV/EHU, E-48080 Bilbao, Spain*
[3]*IKERBASQUE, Basque Foundation for Science, Alameda Urquijo 36-5, E-48008 Bilbao, Spain*
[4]*Department of Physics, The University of Hong Kong, 0000-0002-6536-5575, Pokfulam Road, Hong Kong*
[5]*Cahill Center for Astronomy and Astrophysics, California Institute of Technology, MS 249-17, Pasadena, CA 91125, USA*
[6]*Department of Physics and Astronomy, Johns Hopkins University, Baltimore, MD 21218, USA*

THE STORY OF SUPERNOVA 'REFSDAL' TOLD BY MUSE*

C. Grillo[1], W. Karman[2], S. H. Suyu[3], P. Rosati[4], I. Balestra[5], A. Mercurio[6], M. Lombardi[7], T. Treu[8], G. B. Caminha[4], A. Halkola, S. A. Rodney[9,10,11], R. Gavazzi[12], K. I. Caputi[2]

Draft version March 7, 2016

Monthly Notices of the ROYAL ASTRONOMICAL SOCIETY
MNRAS 457, 2029–2042 (2016) doi:10.1093/mnras/stw069

Hubble Frontier Fields: predictions for the return of SN Refsdal with the MUSE and GMOS spectrographs

M. Jauzac,[1,2,3]★ J. Richard,[4] M. Limousin,[5] K. Knowles,[3] G. Mahler,[4] G. P. Smith,[6]
J.-P. Kneib,[5,7] E. Jullo,[5] P. Natarajan,[8] H. Ebeling,[9] H. Atek,[8] B. Clément,[4]
D. Eckert,[10] E. Egami,[11] R. Massey[1,2] and M. Rexroth[7]

of MACS J0416.1−2403 and Abell 2744. In light of the discovery of the first resolved quadruply lensed supernova, SN Refsdal, in one of the multiply imaged galaxies identified in MACS J1149, we use our revised mass model to investigate the time delays and predict the rise of the next image between 2015 November and 2016 January.

Supernova em MACS J1149.6+2223

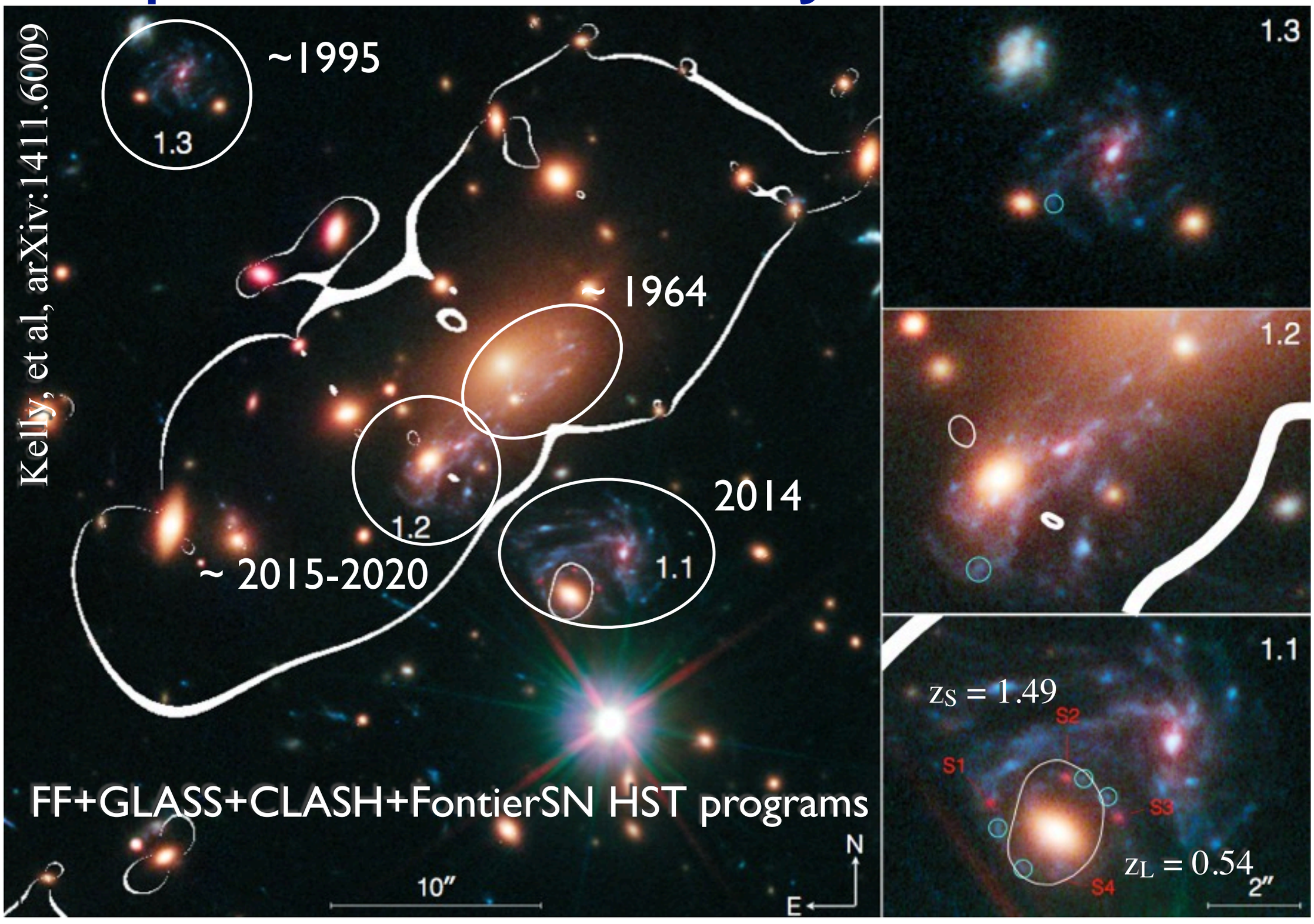

DEJA VU ALL OVER AGAIN: THE REAPPEARANCE OF SUPERNOVA REFSDAL

P. L. Kelly[1], S. A. Rodney[2], T. Treu[3,3], L.-G. Strolger[4], R. J. Foley[5,6], S. W. Jha[7], J. Selsing[8], G. Brammer[4], M. Bradač[9], S. B. Cenko[10,11] Show full author list

Published 2016 February 24 • © 2016. The American Astronomical Society. All rights reserved.

The Astrophysical Journal Letters, Volume 819, Number 1

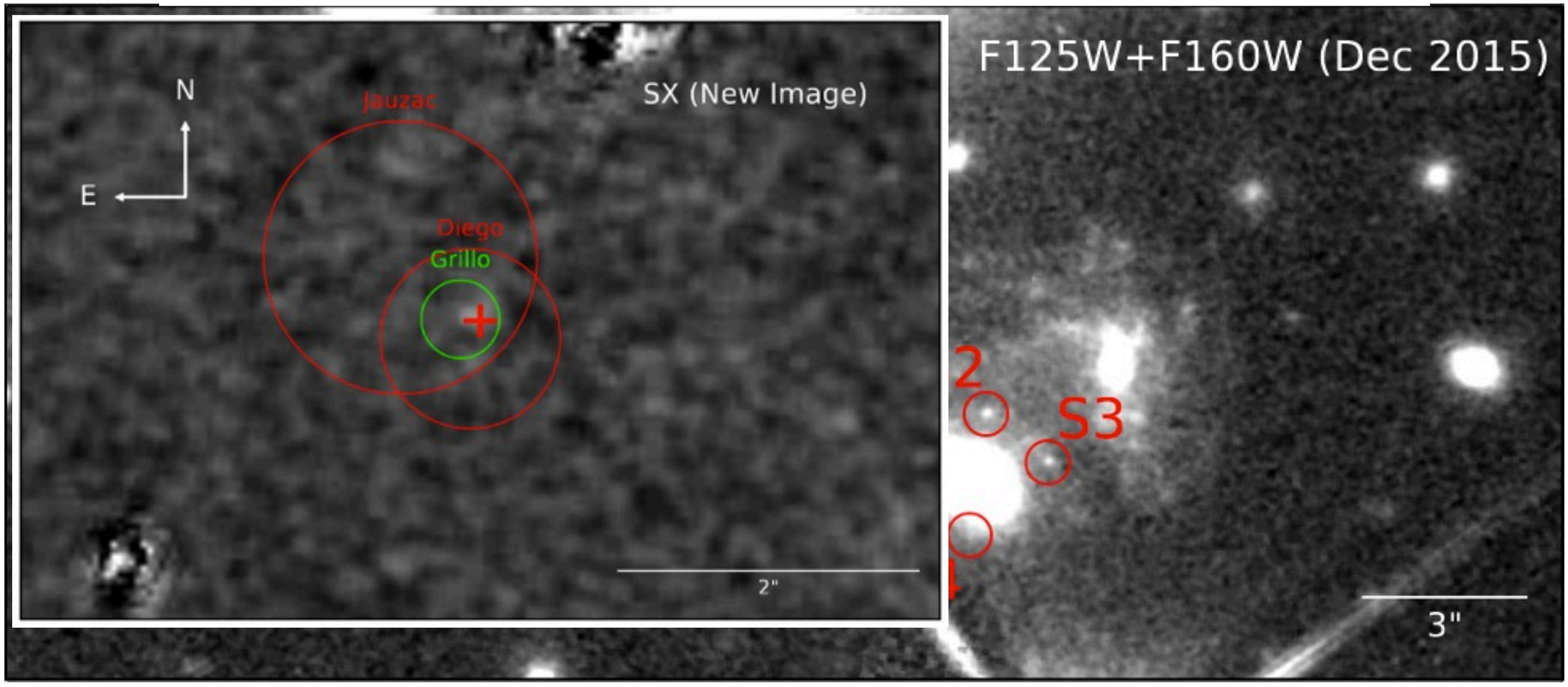

Dark Energy from Families of Multiple Images

Galaxy Cluster Scale
Cosmological Constraints and more

$$\vec{\theta} = \vec{\beta} + \frac{2}{c^2}\frac{D_{LS}}{D_{OS}D_{OL}}\nabla_\theta \psi\left(\vec{\theta}\right)$$

Families of images with sources at different *redshifts*

☑ constraints on cosmology, in addition to the matter distribution

The ratio of angular diameter distances for 2 (or more) images with sources at different redshifts defines a ratio of families

$$\Xi(z_{\rm l}, z_{\rm s1}, z_{\rm s2}; \Omega_{\rm M}, \Omega_{\rm X}, w_{\rm X}) = \frac{D(z_{\rm l}, z_{\rm s1})}{D(0, z_{\rm s1})}\frac{D(0, z_{\rm s2})}{D(z_{\rm l}, z_{\rm s2})}$$

☑ Jullo et al. 2010, Science: example of competitive limits in cosmological parameters fom the Abell 1689 system

☑ **8** families of sources with z = 1.15 to 4.86

☑ Caminha et al. 2016: RXC J2248.7-4431 (Abell S1063), 16 sources, 47 images

☑ Magaña, Motta, Cárdenas, Verdugo, Jullo, 2015

Angular Diameter Distance

Flat case:

$$D_A(0,z) = \left(1+z\right)^{-1} \int_0^z \frac{dz'}{H\left(z'\right)}$$

Recall that (in the ΛCDM model)

$$H^2\left(a\right) = H_0{}^2 \left[\Omega_r a^{-4} + \Omega_M a^{-3} + \Omega_k a^{-2} + \Omega_\Lambda\right]$$

and

$$D_A(z_1,z_2) = \frac{\left(1+z_2\right)^{-1}}{H_0} \int_{z_1}^{z_2} \frac{dz'}{\sqrt{\Omega_r\left(1+z'\right)^4 + \Omega_M\left(1+z'\right)^3 + \Omega_\Lambda}}$$

$$D_{LS} = D_A(z_L, z_S)$$

© Copyleft Martín Makler

Cosmological Constraints

Frontier Field Cluster AS1063 (aka RXJ2248)

Caminha et al., 2016

MUSE SV programme + GO (PI: K.Caputi)
(Karman et al. 2015)
(W.Karman et al. 2016, arXiv/160601471)

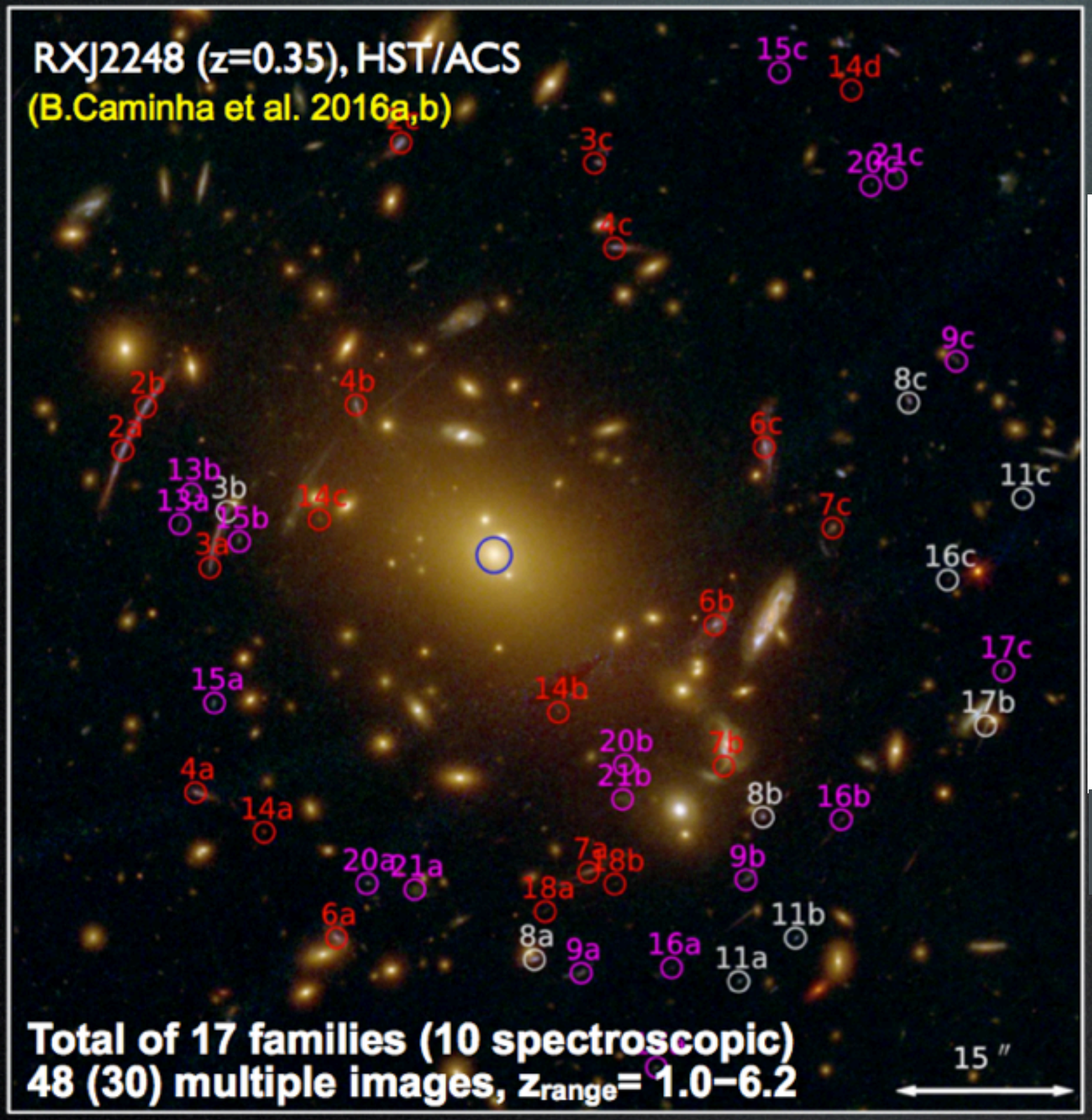

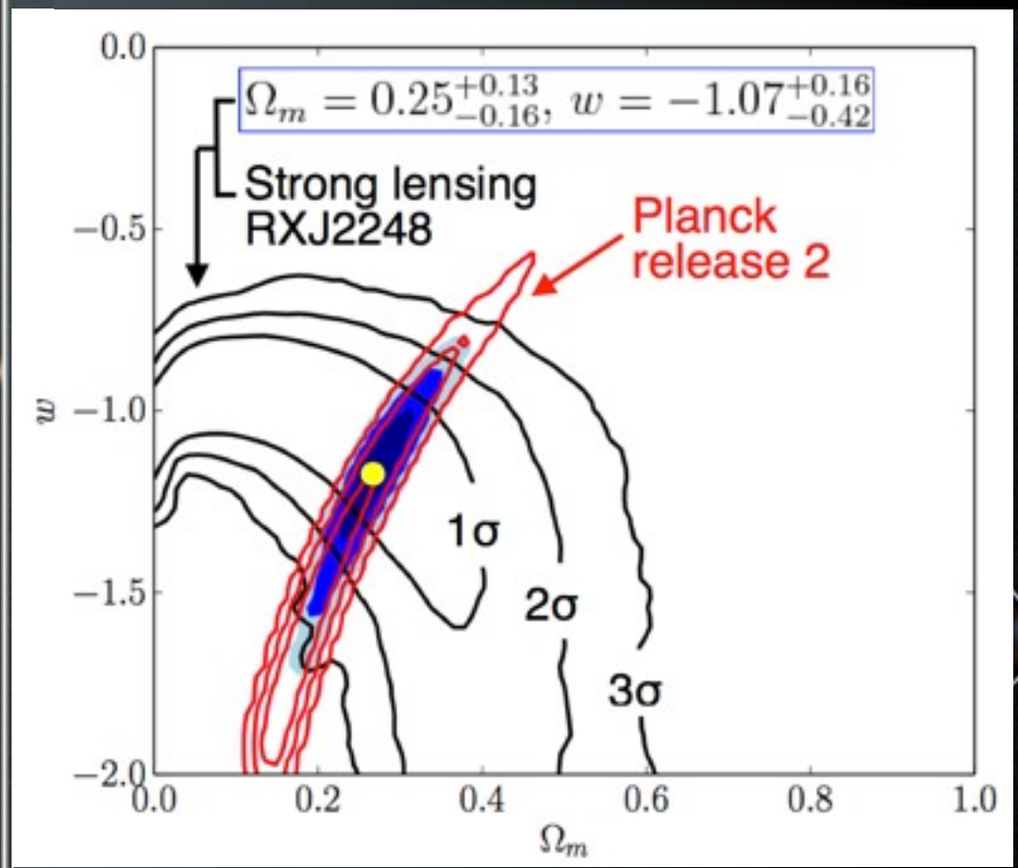

1 arcmin² FoV
2.6 Å resolution (4800-9300 Å)
0.2 arcsec/pxl
Exp. = 5 hrs

New constraints from RXC J2248.7−4431

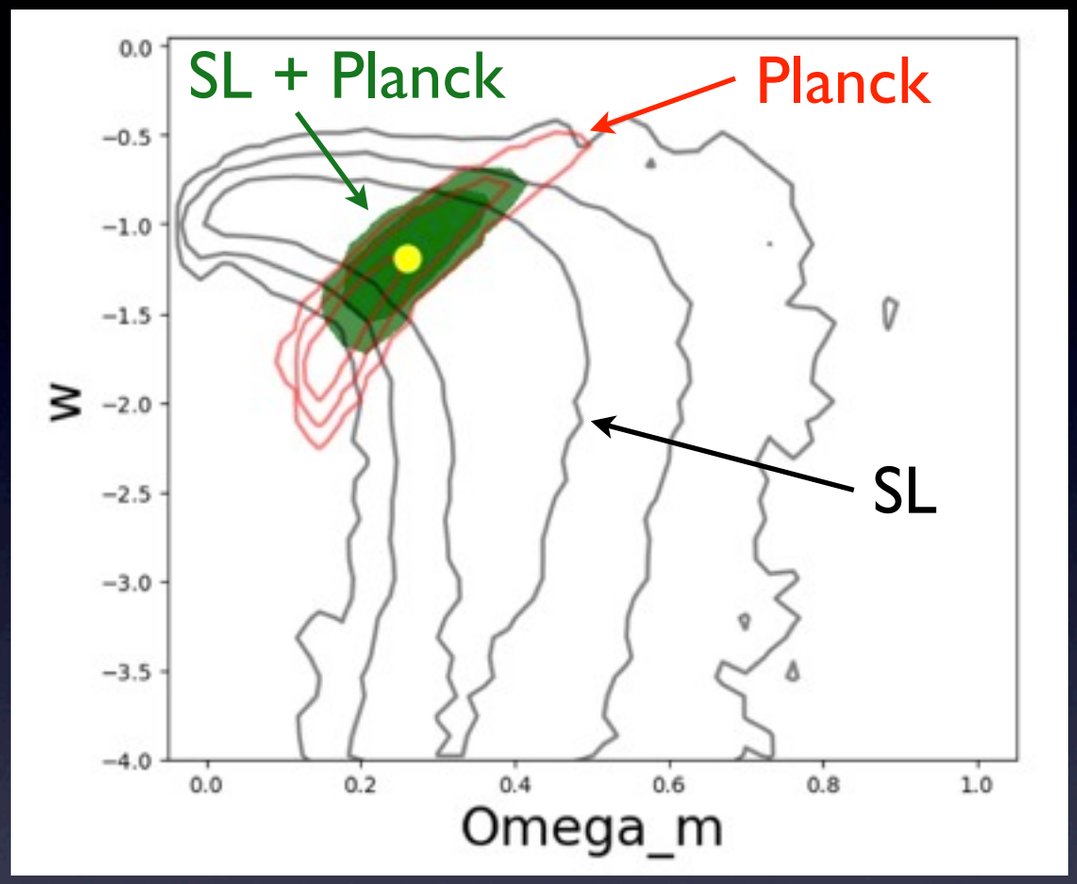

C. Bom, G. Caminha, MM, 2017

HFF: magAB ~ 29, 7 filters + MUSE
(including 5 new families)

Distance ratios from the ground?

Example: RXC J2248.7−4431

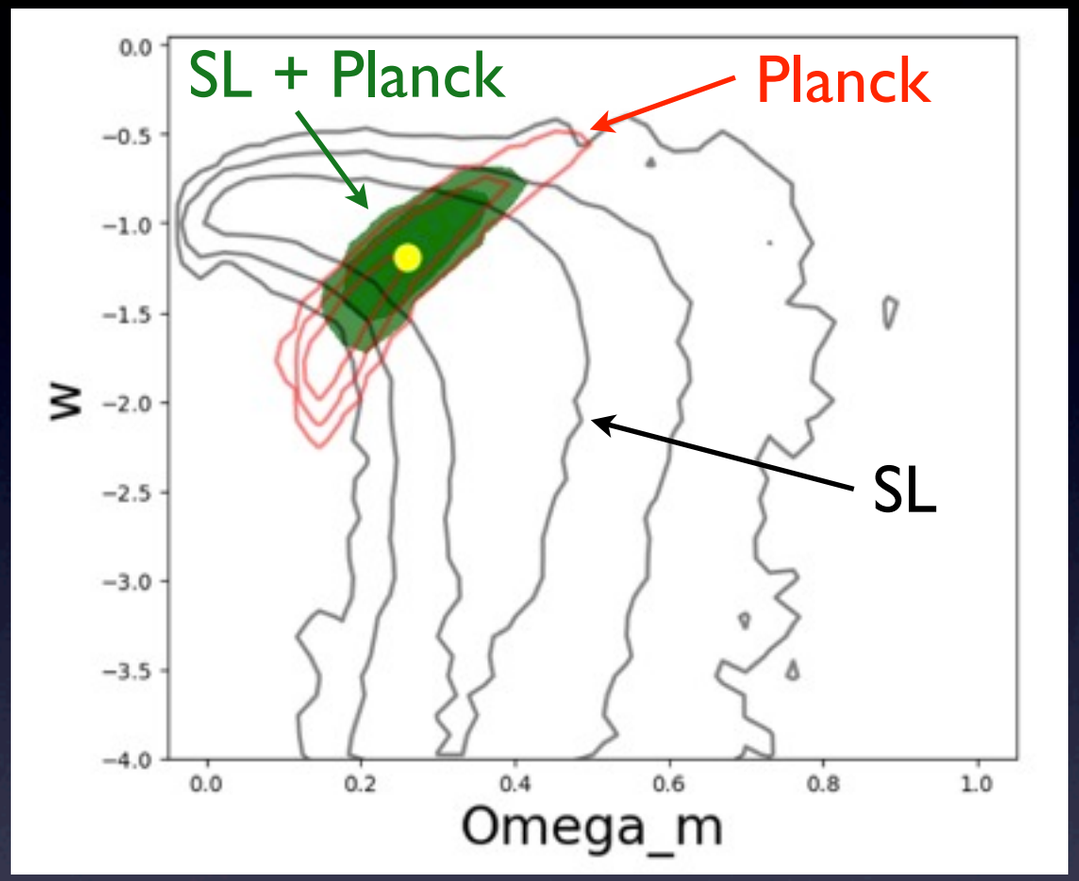

C. Bom, G. Caminha, MM, 2017

HFF: magAB ~ 29, 7 filters + MUSE (including 5 new families)

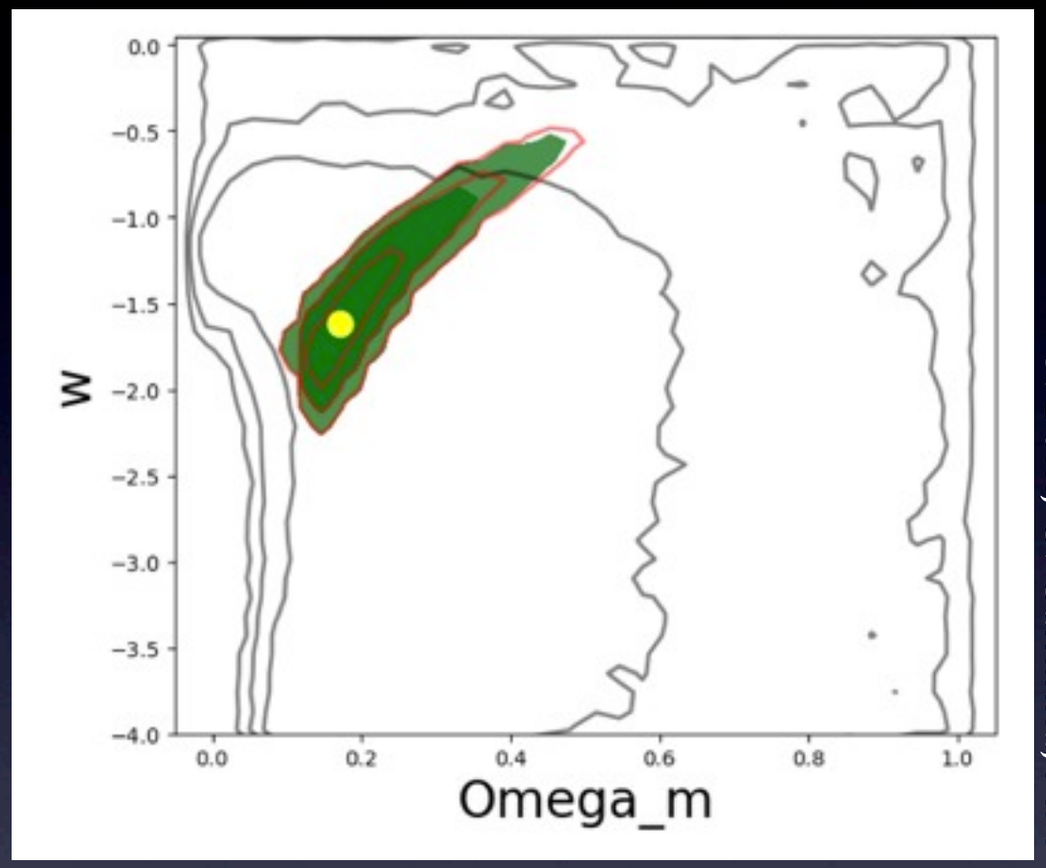

C. Bom, G. Caminha, MM

HFF degraded to FWHM = 0.6”, mag = 25 (7 families, 17 multiple images), assuming known redshifts

- ~ 20 systems would yield the same constraints
- Better for systematics and comparison to simulations

Strong Lensing and Dark Matter

- Large-scale Geometry
  - Background cosmology: Ω_M
- Lens potential: Mass distribution
  - Dark Matter abundance and distribution
  - Primordial spectrum (mass)
  - Self-interaction
- Gravitational telescope
  - z ~ 2 – details of highly magnified galaxies (resolved!)
  - z ~ 6 – galaxy abundance at high-z
- Challenges:
  - High-resolution, deep imaging; spectroscopy (including IFU)
  - Finding Strong Lenses (specially "golden lenses")
  - Systematics

Direct detection of substructure in clusters

Sub-halo power spectrum:

- Quantifying substructures in HFF

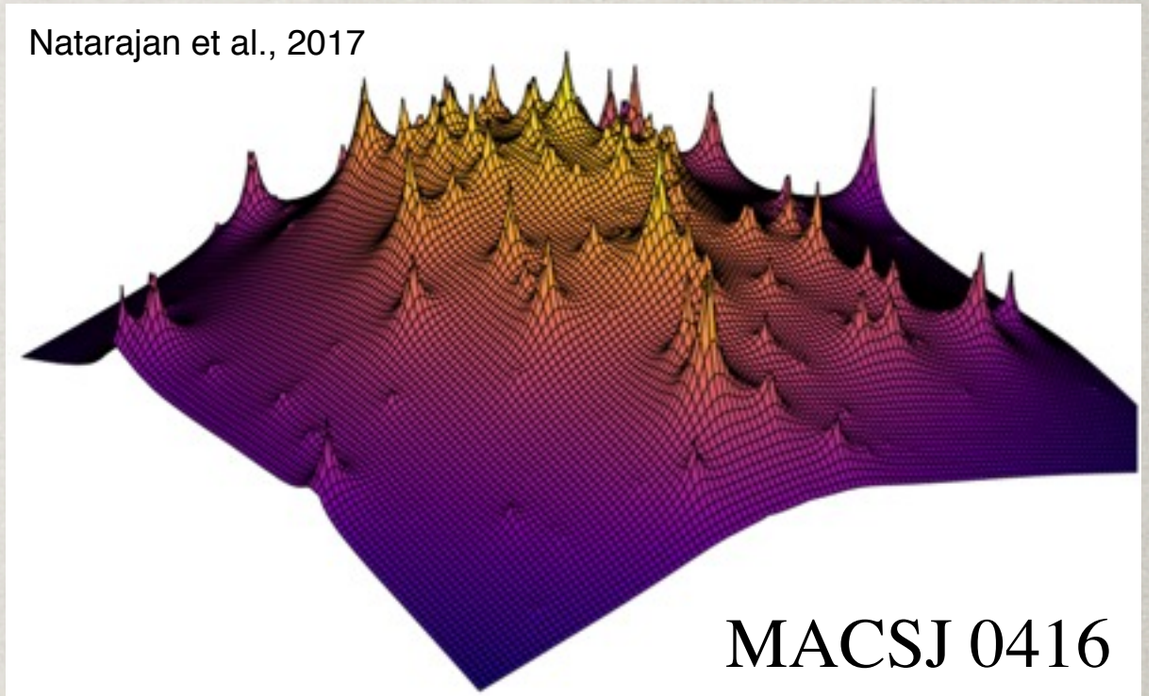

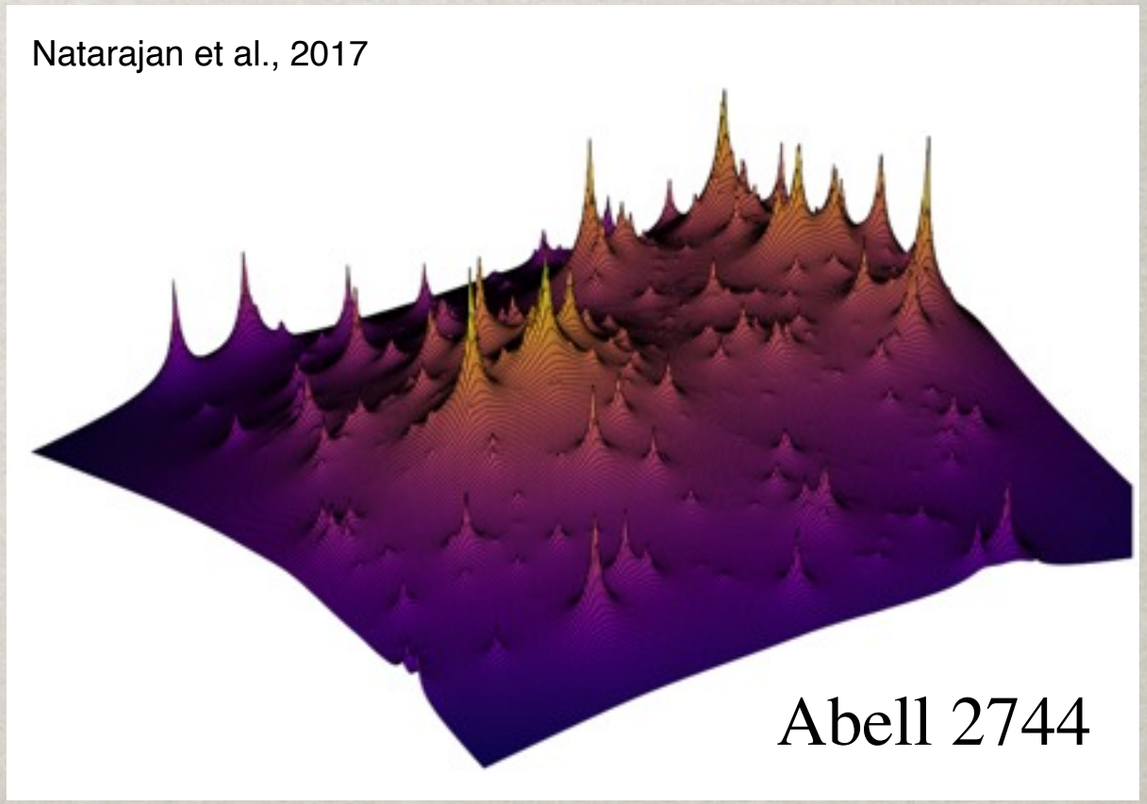

Direct detection of substructure in clusters

Sub-halo power spectrum:

- Quantifying substructures in HFF
- Free form modeling: smaller power
- Evidence for WDM (Mohammed et al. 2016)
- Parametric (LTM) finds excess power: upper limit on self-interaction (Jauzac, M., et al., 2016)
- Free form agrees with LTM up to ~ 10 kpc (Sebesta et al. 2016) [139 lensed images]

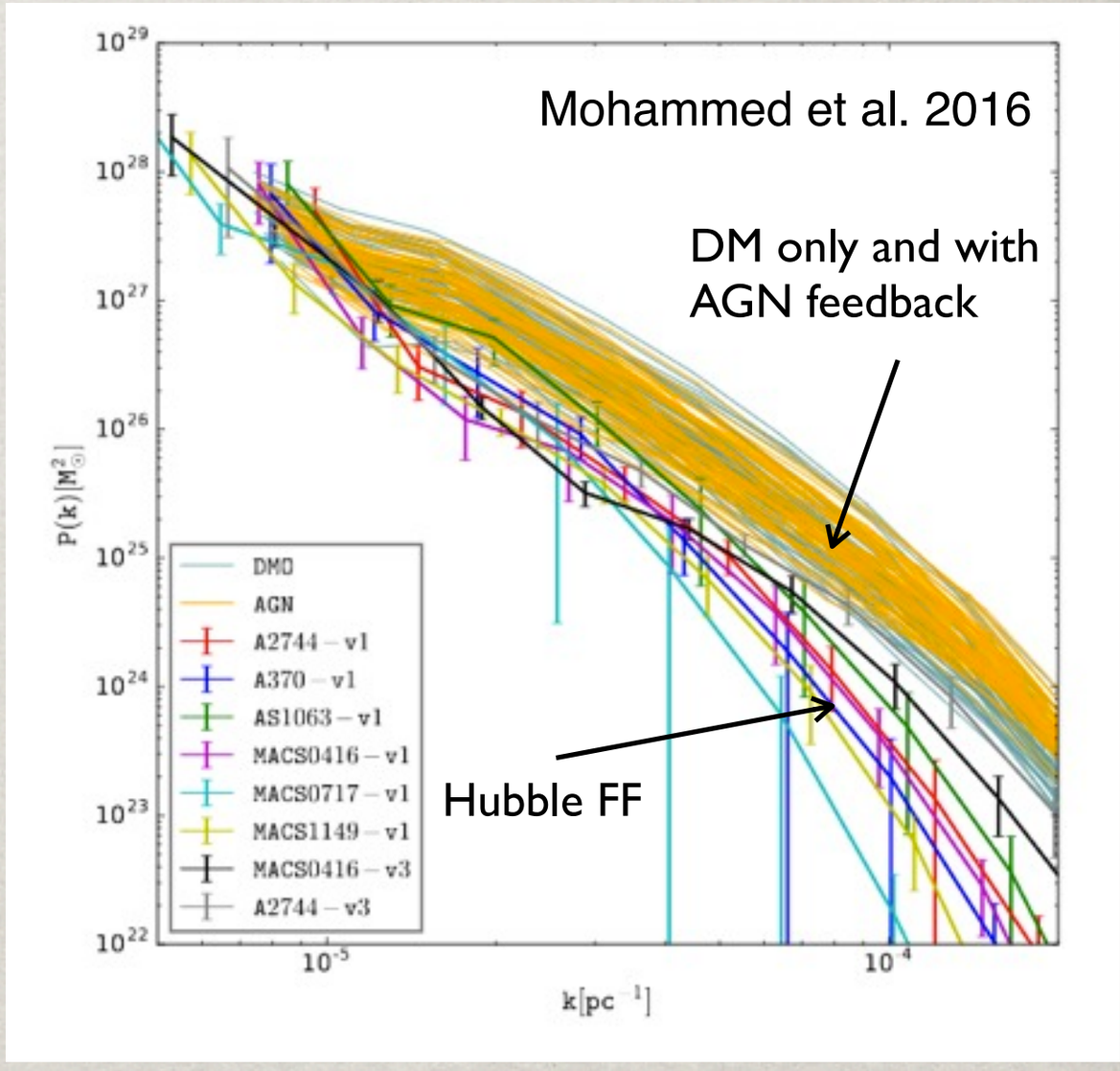

Light-Matter Offsets

- Self-Intercting Dark-Matter predicts offsets between luminous and dark matter in dense regions: Smoking gun for SIDM
- Williams and Saha (2011): *kpc*-scale offsets in Abell 3827 from Free form modeling -> lower limit in cross section
- Mohamed et al. (2014): Abell 3827 and also Abell 2218, no LoS
- Schaller (2015): tension with CDM
- Harvey et al. (2015), 347, 1462; arXiv:1503.07675, upper limit on SIDM
- Kahlhoefer, et al. (2015), Wittman et al. (2017): constraints overestimated

$$\sigma_{DM}/m_{DM} \lesssim 2\,\mathrm{cm}^2/\mathrm{g}$$

- Monteiro-Oliveira, et al. 2017: simulations (CDM + gas + galaxies)
- Interacting systems. Not seen in field galaxies and relaxed clusters

Galaxy Scale Lenses

- Self-Intercting Dark-Matter predicts offsets between luminous and dark matter in dense regions
  - Seen in clusters, e.g., Harvey et al., 2015, *The nongravitational interactions of dark matter in colliding galaxy clusters*, Science, 347, 1462 (2015); arXiv: 1503.07675
- offsets found in a galaxy scale system
  - Interacting systems
  - kpc offsets in SDSS J1011+0143

    (Shu et al. 2015)
  - If interpreted solely as evidence for self-interacting dark matter:

$\sigma_{DM}/m \sim (1.7 \pm 0.7) \times 10^{-4}\ cm^2\ g^{-1} \times (t_{infall}/10^9\ yr)^{-2}$

  - only SDSS spectroscopy

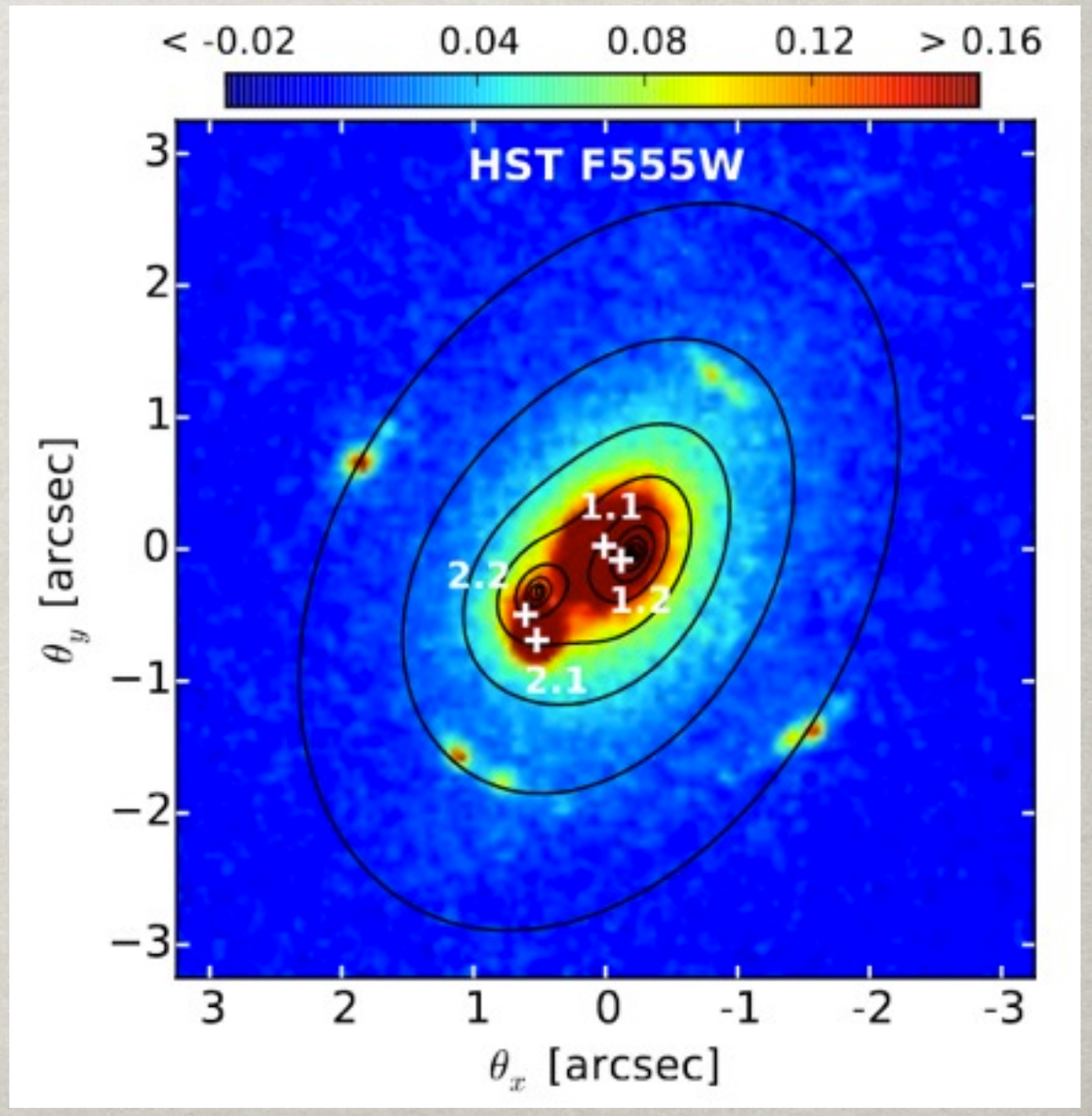

Test on CS82 Einstein Rings?

- Extensive search found 4 excellent Eintein ring candidate systems. One has a double component lens!

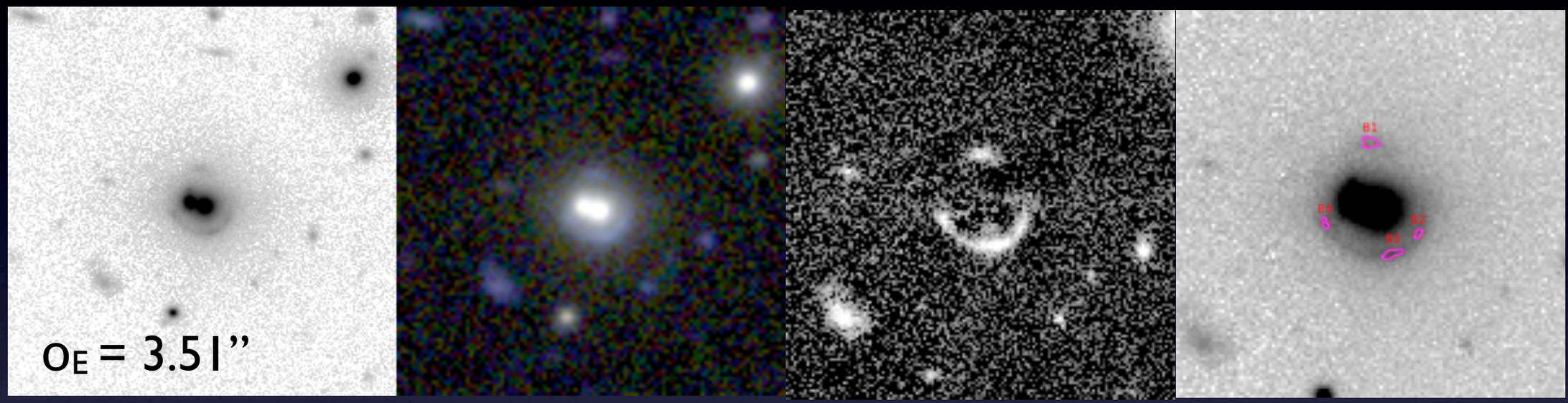

Anna Niemiec

- SDSS (right component), z_{spec} = 0.344, $\sigma_v^{\mathrm{BCG}} = 372 \pm 29$
- Fits with a single and two mass components: evidence for single potential ➔ “bullet cluster like”?
- velocity dispersion (from SL): 440 km/s
- Need to fit brightness distribution
- SOAR follow-up next September!

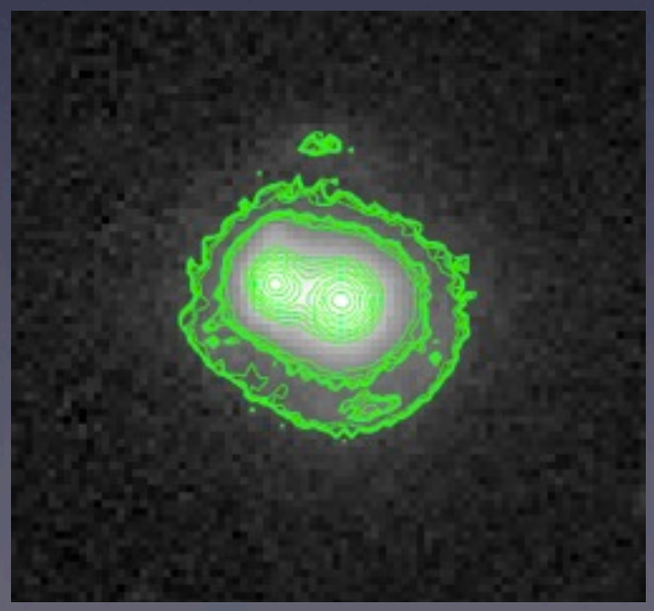

Gravitational telescopes: luminosity function of ultra-fraint UV galaxies at high-redshift

- Warm Dark Matter produces a cutoff in the matter power spectrum (Bode et al. 2001) and thus on the halo mass function

A STRINGENT LIMIT ON THE WARM DARK MATTER PARTICLE MASSES FROM THE ABUNDANCE OF $z = 6$ GALAXIES IN THE HUBBLE FRONTIER FIELDS

N. Menci[1], A. Grazian[1,2], M. Castellano[1], and N. G. Sanchez[3]

Published 2016 June 23 • © 2016. The American Astronomical Society. All rights reserved.
The Astrophysical Journal Letters, Volume 825, Number 1

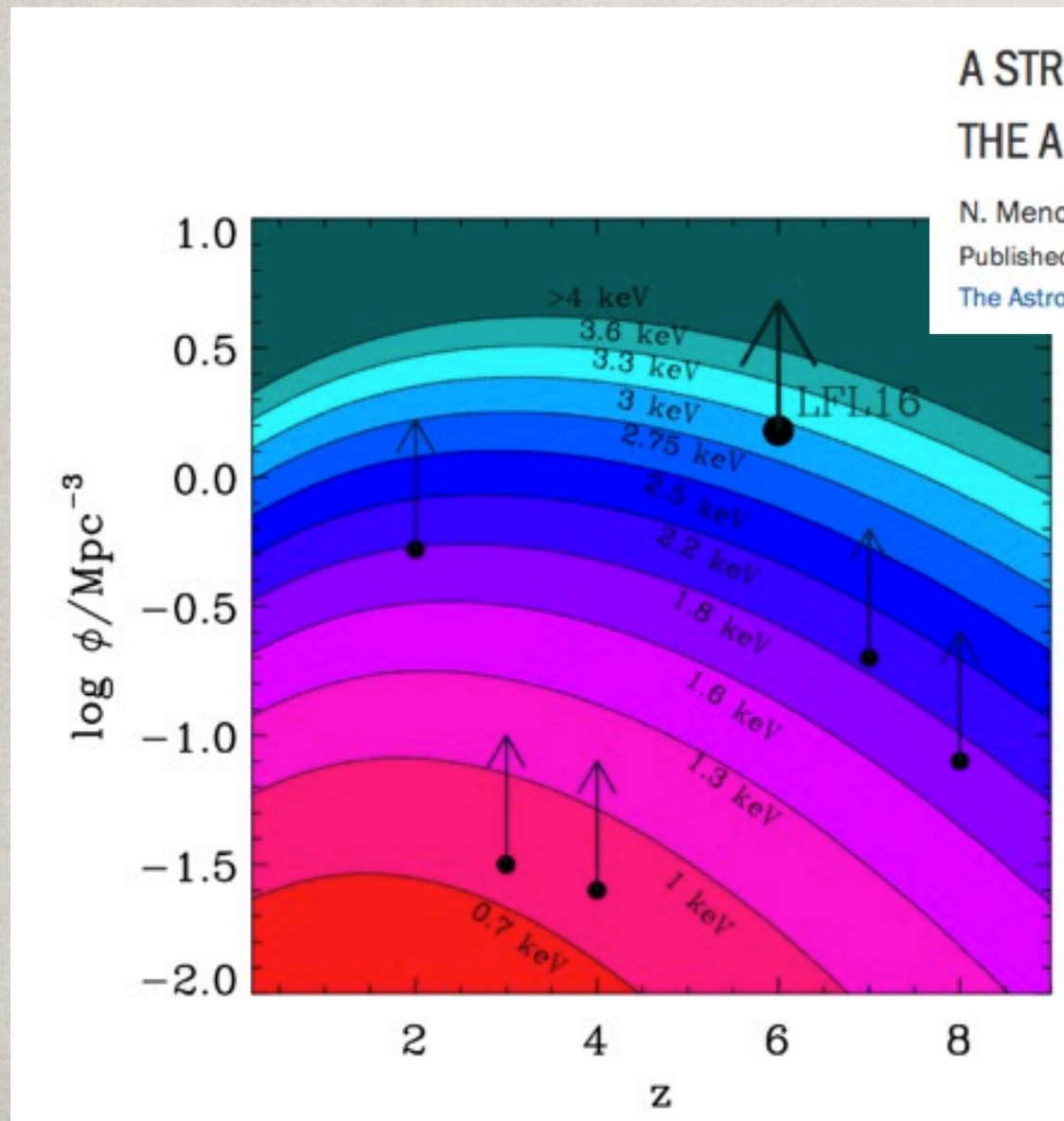

Mass of thermal relic WDM particles $m_X \geq 2.1$ keV at 3σ.

- Need to take into account uncertainties and systematics in the magnification
- Priewe, et al. 2017, Bouwens, et al. 2017

Galaxy Scale Lenses

- Einstein rings
  - Probing mass profiles
  - Modified gravity
  - HST (SLACS/BOSS), CFHTLS
- Time delays
  - H_0, time delay distance
  - Angular diameter distance
  - HST mass models
  - Supernovae!

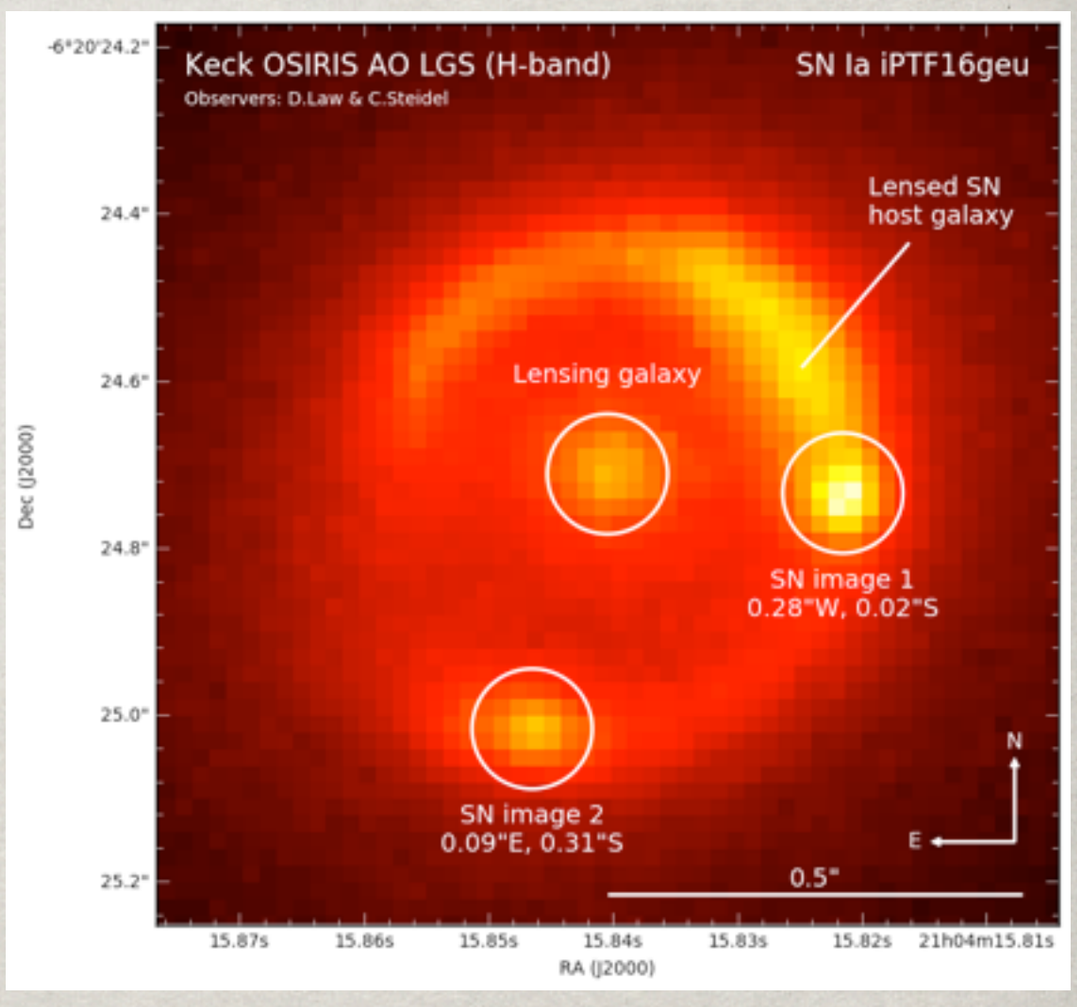

Goobar et al., The discovery of the multiply-imaged lensed Type Ia supernova iPTF16geu, arXiv:1611.00014

Strong Lensing and Modified Gravity

Bending of light by gravity

Null geodesic,
Fermat principle

$$ds^2 = \left(1 + \frac{2\phi}{c^2}\right) c^2 dt^2 - \left(1 - \frac{2\phi}{c^2}\right) d\sigma^2$$

$$\frac{d\sigma}{dt} := c' = \sqrt{\frac{1 + 2\phi/c^2}{1 - 2\phi/c^2}} \simeq c(1 + 2\phi/c^2)$$

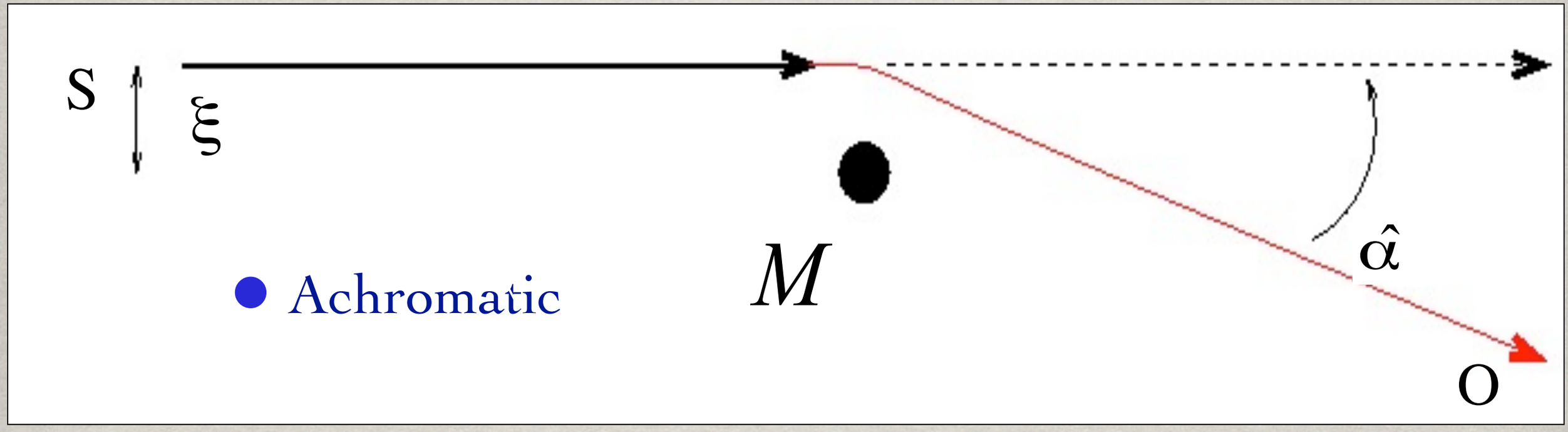

- Achromatic

Deflection angle (point source) $\hat{\alpha} = \frac{4GM}{c^2}\frac{1}{\xi}$

Bending of light by (modified) gravity

Null geodesic,
Fermat principle

$$ds^2 = \left(1 + \frac{2\psi}{c^2}\right) c^2 dt^2 - \left(1 - \frac{2\phi}{c^2}\right) d\sigma^2$$

peculiar gravitational potentials
(in GR $\psi = \phi$)

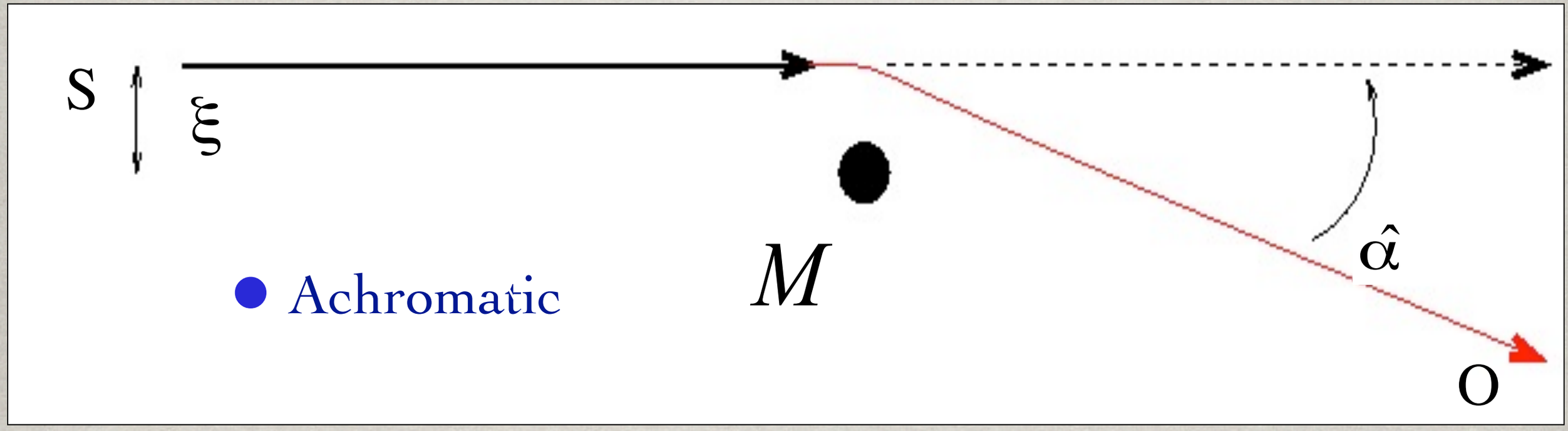

- Achromatic

Bending of light by (modified) gravity

Null geodesic,
Fermat principle

$$ds^2 = \left(1 + \frac{2\psi}{c^2}\right) c^2 dt^2 - \left(1 - \frac{2\phi}{c^2}\right) d\sigma^2$$

$$\frac{d\sigma}{dt} = c' = c\sqrt{\frac{1 + \frac{2\psi}{c^2}}{1 - \frac{2\phi}{c^2}}} \simeq c\left(1 + \frac{\psi + \phi}{c^2}\right) \qquad \frac{\phi}{\psi} = \gamma$$

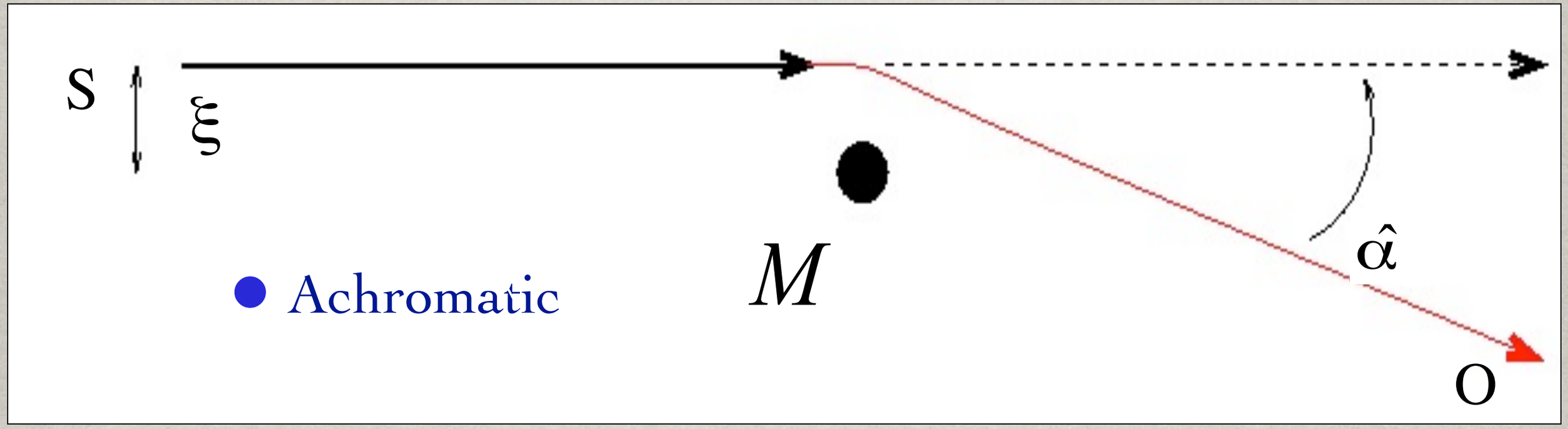

- Achromatic

Dynamical mass obtained from

$$\nabla^2\psi = 4\pi G\rho$$

Use combination of lensing + dynamics to test gravity

Einstein Rings

Einstein Ring $$R_E = 4\pi\sigma_{\rm obs}^2 \left(\frac{1+\gamma_{\rm PPN}}{2}\right) \frac{D_L D_{LS}}{D_S}$$

Measure velocity dispersion ➔ Limit on gravity

Einstein rings in the SLACS sample

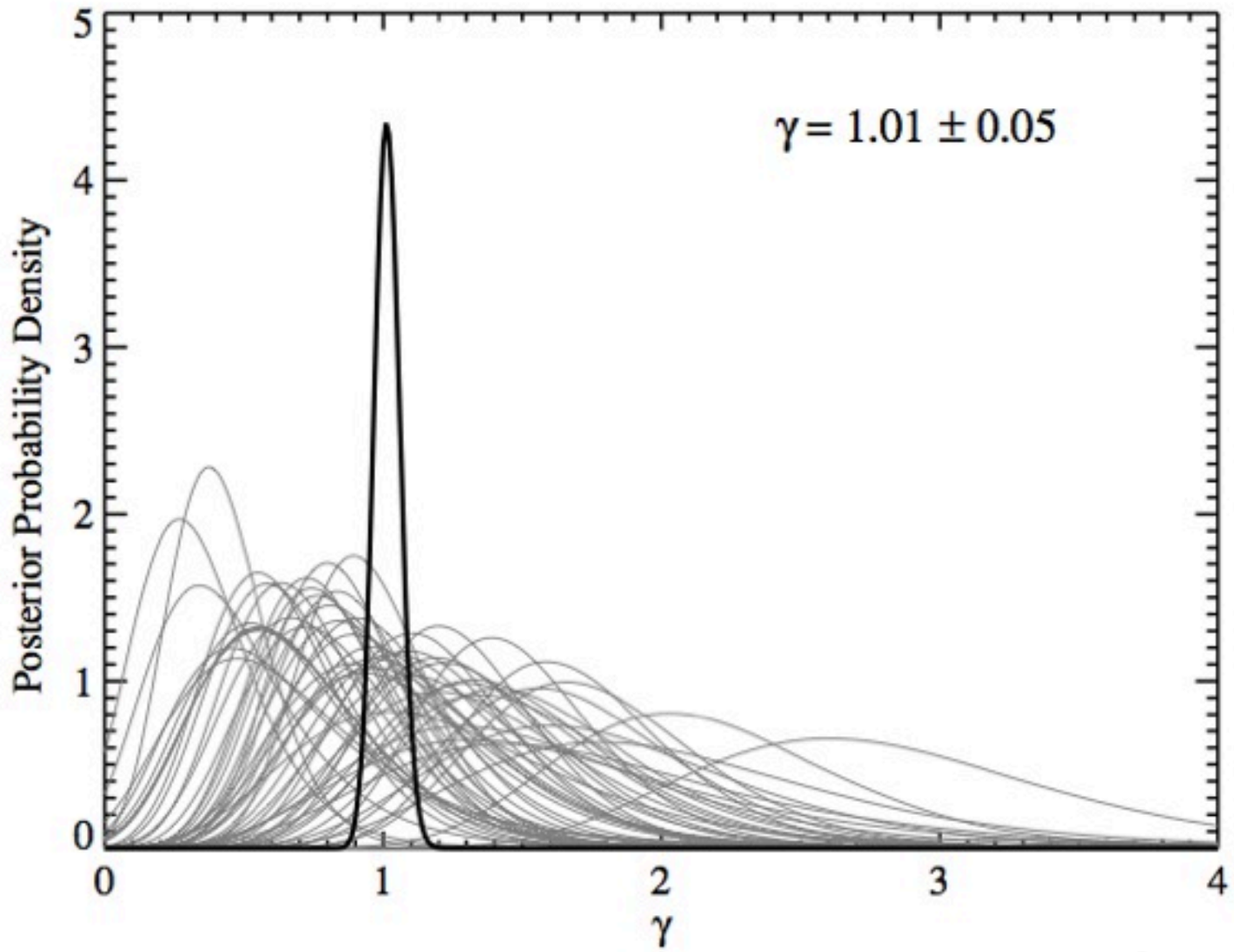

Schwab, Bolton, Rappaport, arXiv:0907.4992; Smith, arXiv:0907.4829;

The results are in agreement with GR

Time Delays and Cosmology

Time delay

Geometric + gravitational redshift + Doppler (observer frame)

$$\delta t_L = \delta t_{\rm geom} + \delta t_{\rm grav}$$

$$\delta t_{\rm geom} = \delta L/c = \frac{D_{OS} D_{OL}}{2 c D_{LS}} (\vec{\theta} - \vec{\beta})^2 \qquad \delta t_{grav} = -\frac{2}{c^3}\psi$$

$$\delta_{t_O}/\delta_{t_L} = a_O/a_L = (1 + z_L) \qquad \Psi \equiv \frac{2}{c^2}\frac{D_{\rm LS}}{D_{\rm OS} D_{\rm OL}}\psi$$

$$\delta t = (1 + z_L)\frac{D_{OS} D_{OL}}{c D_{LS}} \left(\frac{1}{2}(\vec{\theta} - \vec{\beta})^2 - \Psi \right)$$

$\vec{\nabla}_\theta(\delta t) = 0$ ⇨ **Lens equation!**

Obs.: rigorous derivation at Petters, Levine, Wambsganss

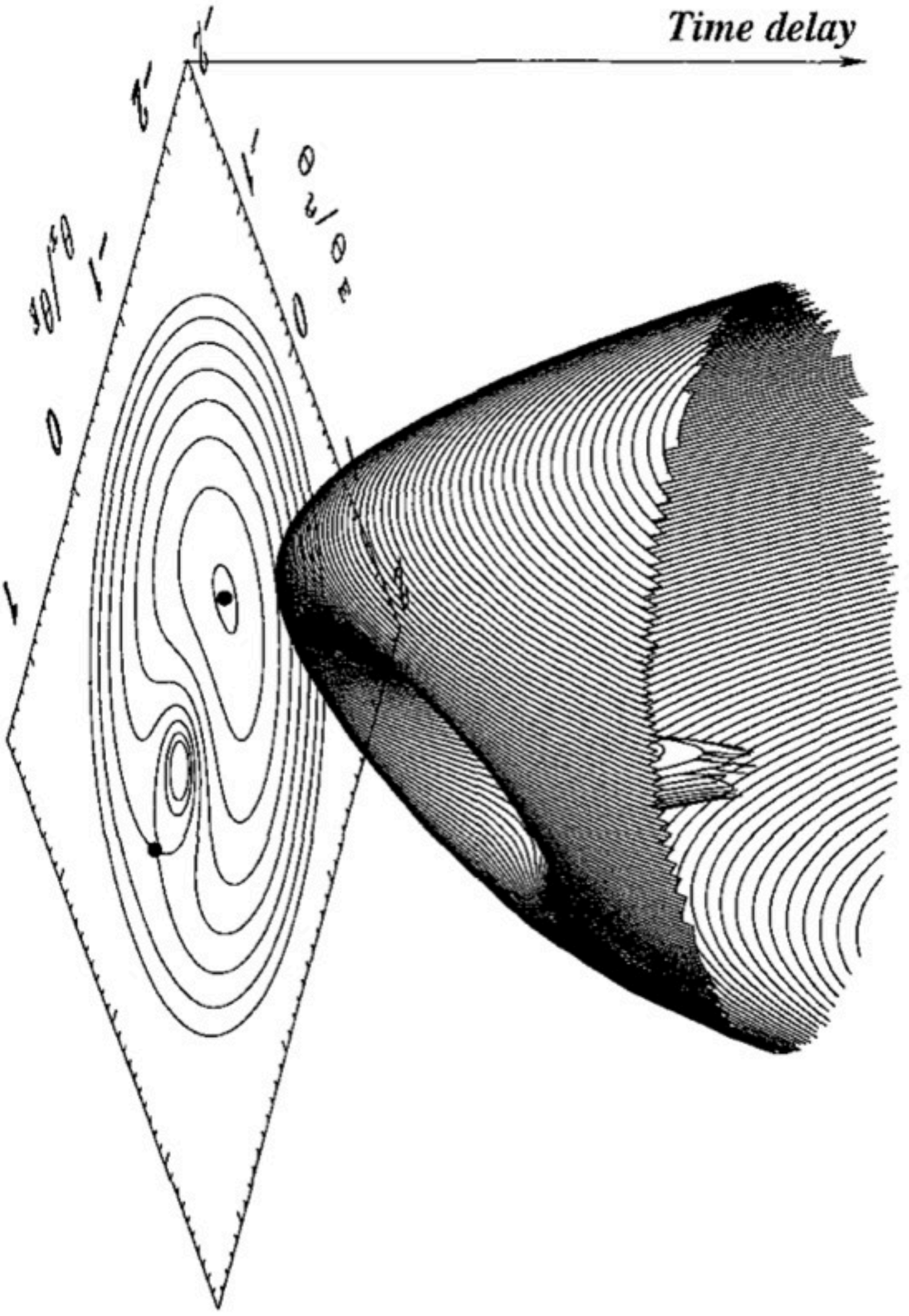
Time delay

Teorema de Burke

1981ApJ...244L...

THE ASTROPHYSICAL JOURNAL, 244:L1, 1981 February 15
© 1981. The American Astronomical Society. All rights reserved. Printed in U.S.A.

MULTIPLE GRAVITATIONAL IMAGING BY DISTRIBUTED MASSES[1]

WILLIAM L. BURKE
Lick Observatory, Boards of Studies in Astronomy and Astrophysics and in Physics, University of California, Santa Cruz, CA 95064
Received 1980 September 26; accepted 1980 November 5

ABSTRACT

A transparent galaxy, not necessarily spherical, acting as a gravitational lens produces an odd number of images.

Subject headings: galaxies: general — gravitation — quasars

In a recent *Letter* (Dyer and Roeder 1980) it was shown that a transparent spherical galaxy of finite mass acting as a gravitational lens produces an odd number of images. The result is in fact true for arbitrary mass distributions as long as the bending (roughly m/r) remains bounded as r goes to infinity. This covers all realizable cases, since larger masses would be within their own event horizons.

A proof of this stronger result is easy. Parametrize the rays leaving the source by their impact parameters (u, v), measured in some plane near the deflector and transverse to the rays. See Figure 1. You may think of this plane as the celestial sphere. The action of the gravitational lens bends a ray. Let us look at the intersection of this bent ray with another transverse plane, this one passing through the receiver. We can measure the bending by the direction cosines (s, w) between two lines: one from the source to the point (u, v) in the deflector plane, and one from that point to the point where the actual ray hits the receiver plane. By a transparent deflector we mean one for which all the rays hitting the first plane also hit the second. This excludes solid objects and black holes.

[1] *Lick Observatory Bulletin*, No. 848.

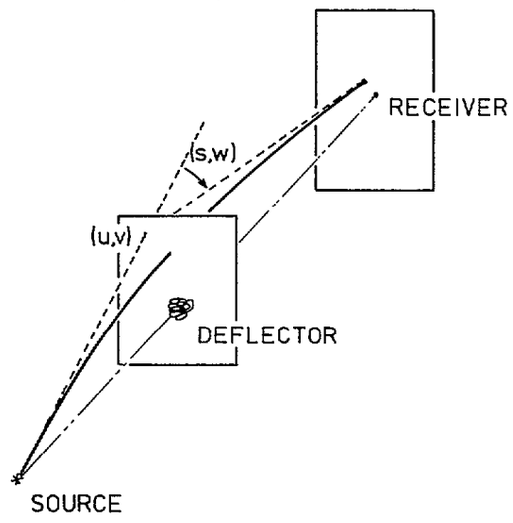

FIG. 1

The action of the gravitational lens is specified by giving the bendings (s, w) as functions of the impact parameters (u, v). Such functions can be represented by a vector field on the (u, v)-plane with components (s, w). A ray with impact parameters (u, v) will reach the receiver only for specific bendings (s, w). This condition can also be represented as a vector field. The gravitational lens will form an image of the source at the receiver whenever these two vector fields are equal.

Subtract these two vector fields. Our problem is to study the zeros of this difference vector field. Since the bending is assumed bounded, for large impact parameter the difference vector field is dominated by the requirement that it takes a large bend for the ray to reach us. For large impact parameter the difference vector field is mainly radial. The zeros of a vector field on the plane are constrained by the Poincaré-Hopf index theorem (see Guillemin and Pollack 1974), which assigns an index to a region by counting the net rotation of the vector field around the boundary of the region. The index of a region is the sum of the indices around the zeros. Simple zeros of a vector field are either sources, sinks, or saddle points. Sources and sinks have index $+1$ and correspond to direct images, while saddle points have index -1 and correspond to inverted images (as in Dyer and Roeder's 1980 Fig. 2). The sum of the indices of the zeros for our difference vector field must be $+1$ because of the behavior at large impact parameter. Thus if there are only simple images, there must be an odd number of them, with one more direct image than inverted images.

Because this is a topological argument the transverse planes need not be flat, the bendings can be measured by angles, tangents, or whatever, and the straight lines need only be straight in some coordinate chart. The (u, v)-plane can be thought of as the celestial sphere of the source or, since rays are reversible, as the celestial sphere of the receiver.

This research was done at the Aspen Center for Physics, and their hospitality and the partial support of the National Science Foundation are gratefully acknowledged.

REFERENCES

Dyer, C. C., and Roeder, R. C. 1980, *Ap. J. (Letters)*, **238**, L67.

Guillemin, V., and Pollack, A. 1974, *Differential Topology* (Englewood Cliffs, N.J.: Prentice-Hall).

Exemplo: RX J1131−1231

- COSMOGRAIL: the COSmological MOnitoring of GRAvItational Lenses
- Curvas de luz + modelo da lente (+"tudo")

$$\kappa_{\rm pl}(\theta_1,\theta_2) = \frac{3-\gamma'}{2}\left(\frac{\theta_{\rm E}}{\sqrt{q\theta_1^2+\theta_2^2/q}}\right)^{\gamma'-1}$$

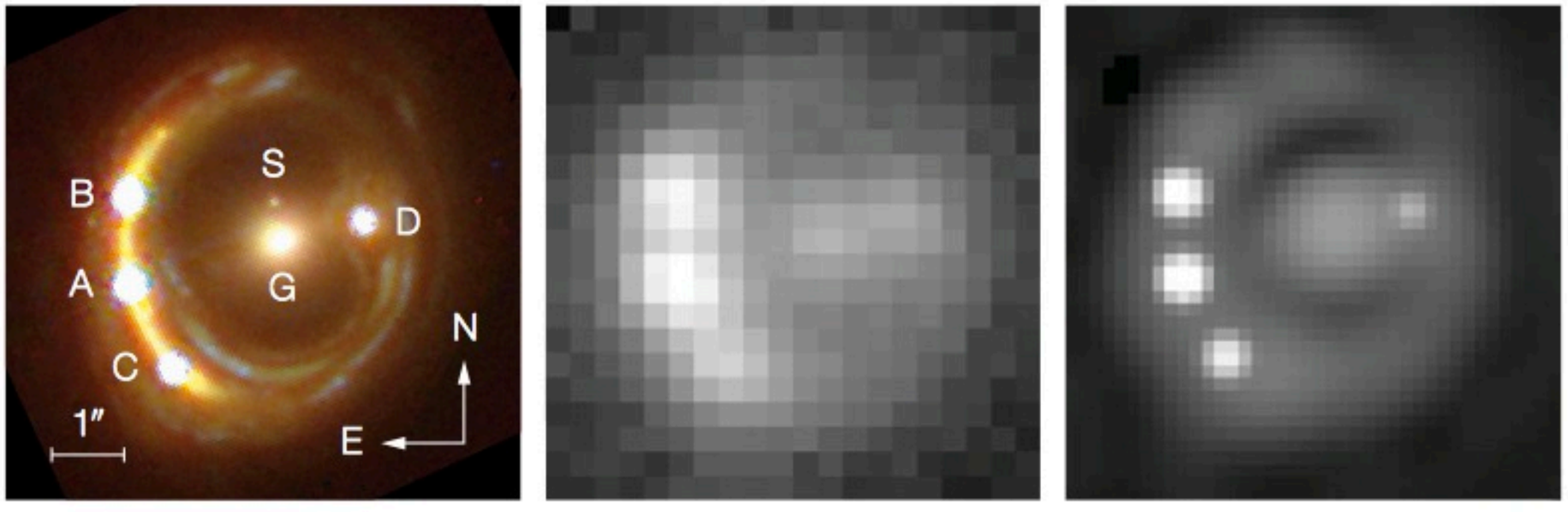

Hubble Space Telescope Swiss Leonhard Euler Telescope Euler deconvolved

Time Delay

$$\Delta t_{ij} = \frac{D_\Delta}{c}\left(\frac{1}{2}(\vec{\theta_i} - \vec{\beta})^2 - \Psi(\theta_i) - \frac{1}{2}(\vec{\theta_j} - \vec{\beta})^2 + \Psi(\theta_j)\right)$$

inverse modeling (multiple images)

Where $D_\Delta = (1 + z_L)\frac{D_{OS} D_{OL}}{D_{LS}}$

"time delay distance"

Main cosmological dependence $\propto H_0^{-1}$

Quasar light-curves

Time delay between images

$$\Delta t_{ij} = \delta t\left(\vec{\theta}_i, \vec{\beta}\right) - \delta t\left(\vec{\theta}_j, \vec{\beta}\right)$$

$$= (1+z_L)\frac{D_{OS}D_{OL}}{cD_{LS}}\left(\frac{1}{2}(\vec{\theta_i} - \vec{\beta})^2 - \Psi(\theta_i) - \frac{1}{2}(\vec{\theta_j} - \vec{\beta})^2 + \Psi(\theta_j)\right)$$

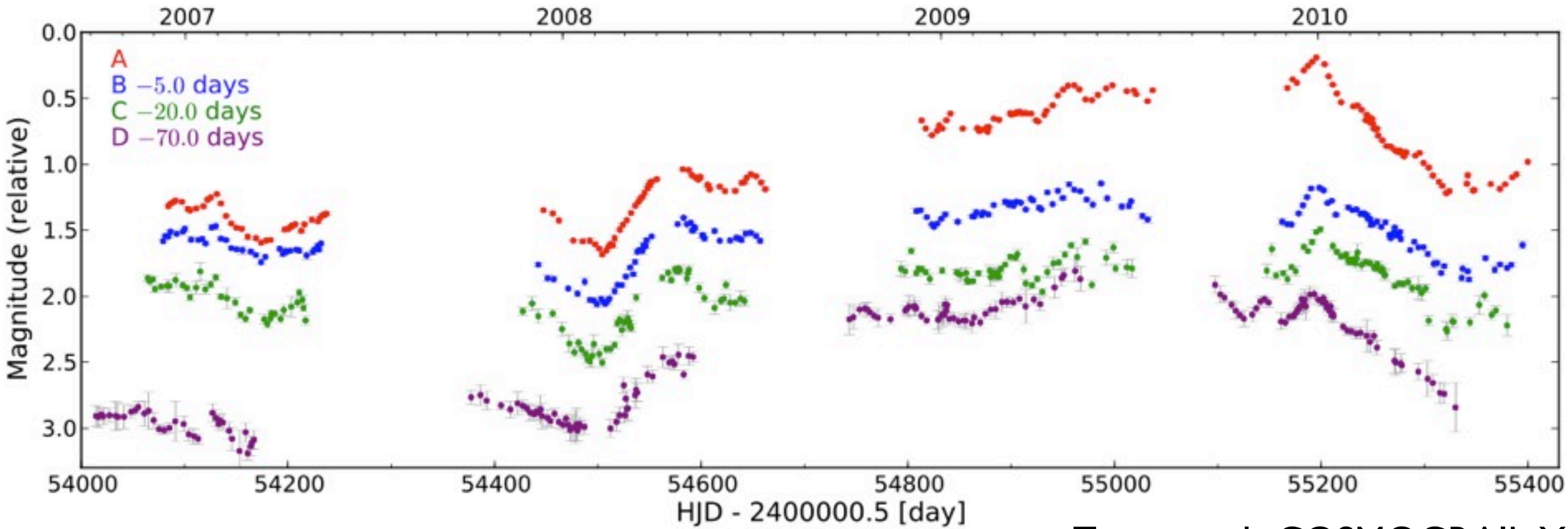

Tewes et al.: COSMOGRAIL XI

Modeling of RX J1131−1231

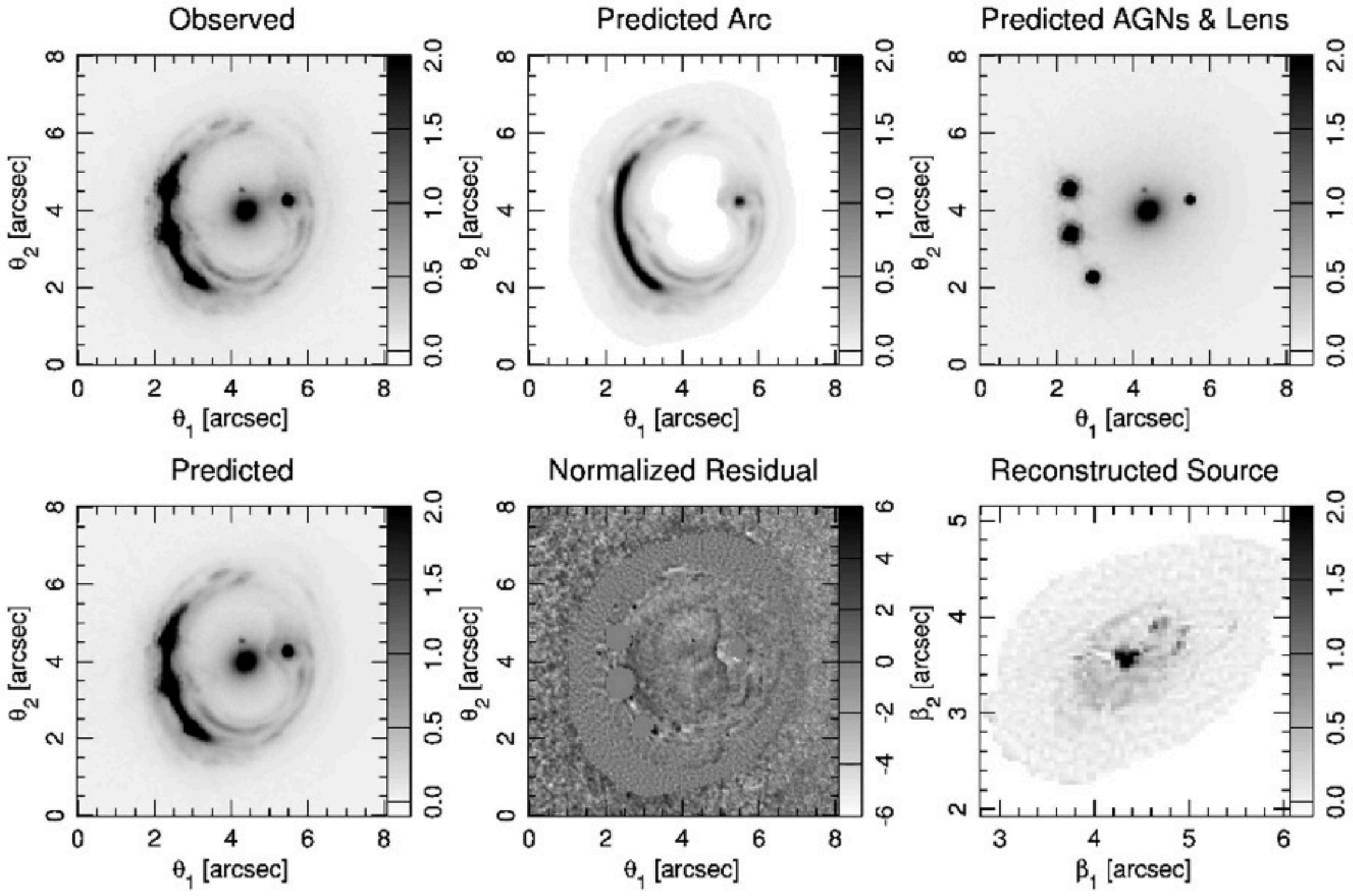

Cosmology Results

Non-flat ΛCDM cosmology
WMAP/Planck for $\{H_0, \Omega_\Lambda, \Omega_m\}$
$\Omega_k = 1 - \Omega_\Lambda - \Omega_m$

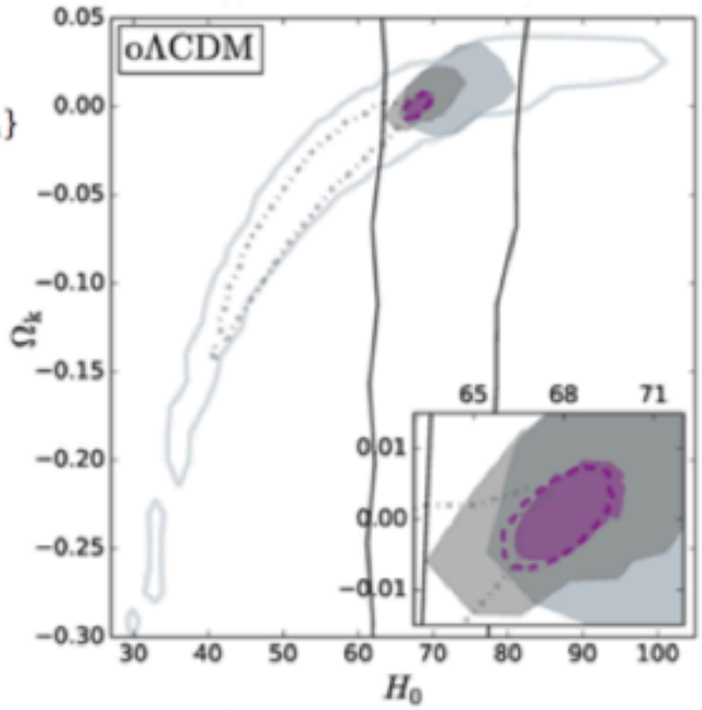

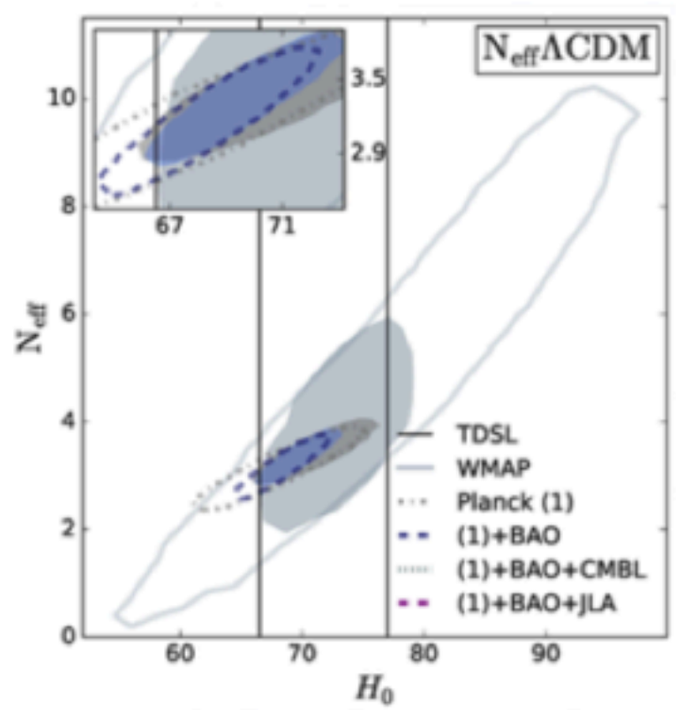

Flat ΛCDM cosmology
WMAP/Planck for $\{H_0, \Omega_\Lambda, \Sigma m_\nu\}$

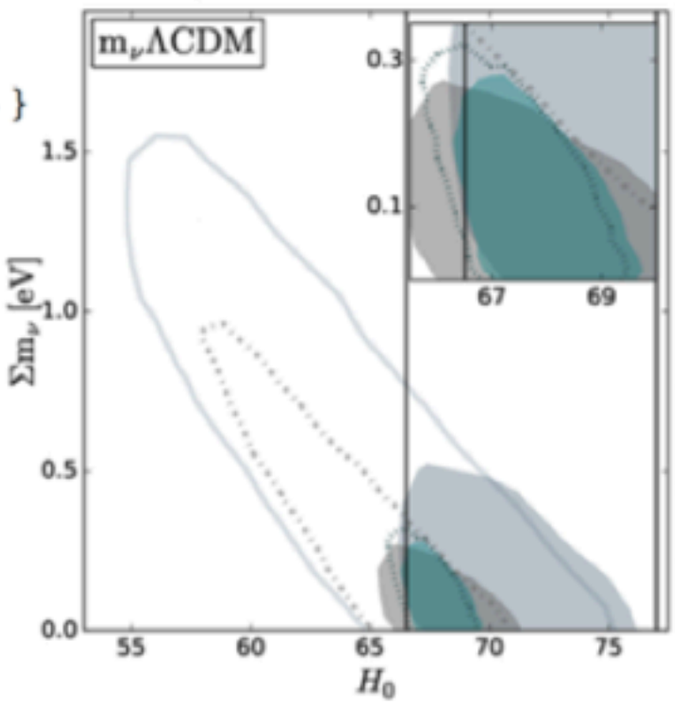

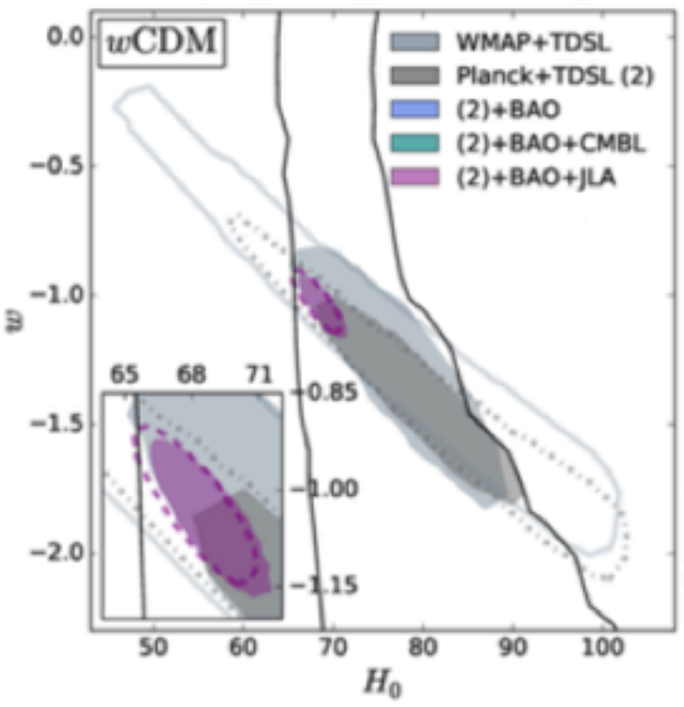

Flat wCDM cosmology
Planck for $\{H_0, w, \Omega_{de}\}$

Bonvin et al. 2016
(Paper V; arXiv:1607.01790)
Cosmology results for 3 lenses

Comparison with other Cosmological Probes

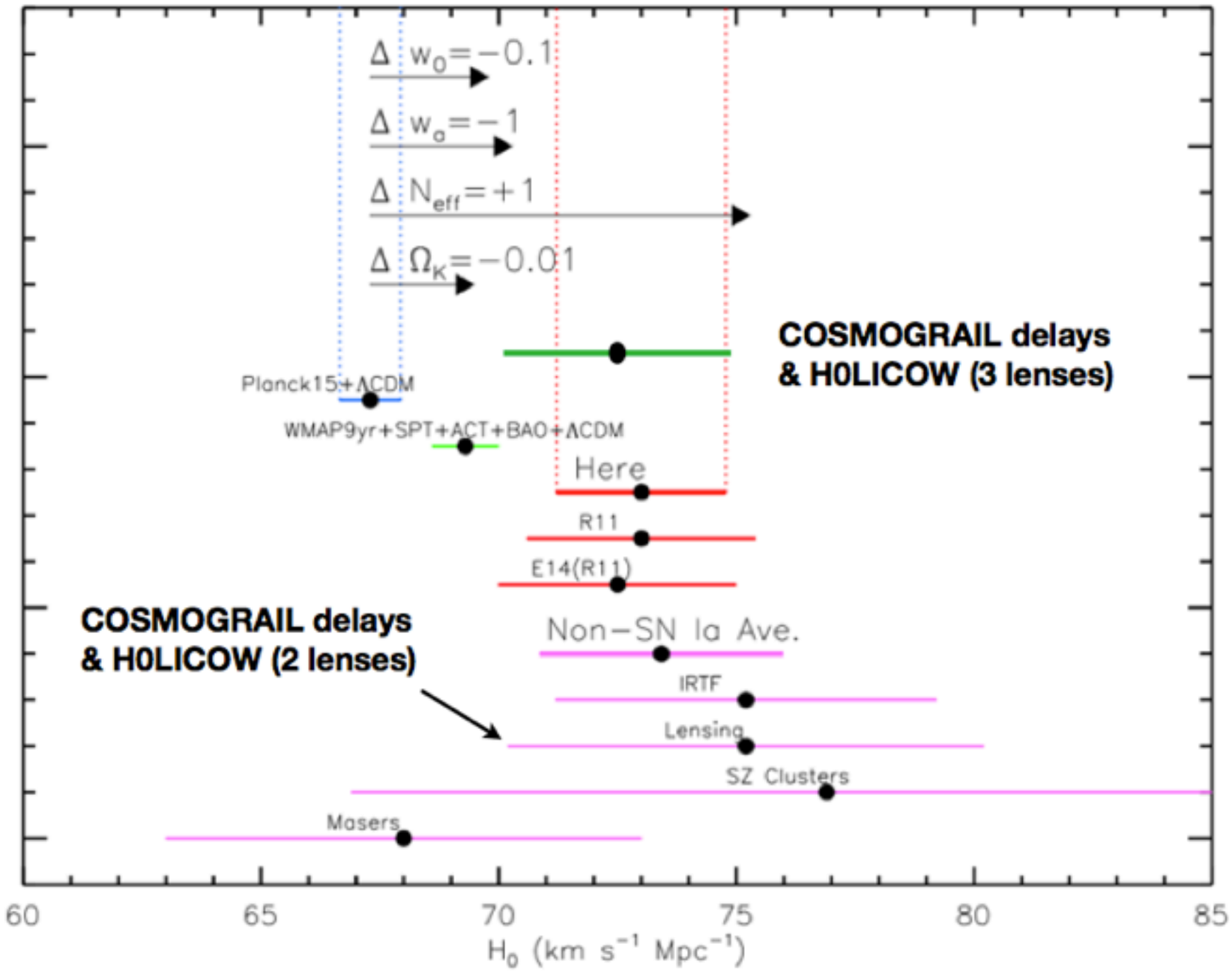

Adapted From Riess et al. (2016)